University of Stavanger

Faculty of Science and Technology

MASTER'S THESIS

Study program/ Specialization: **Masters of Science Environmental Technology/ Offshore Environmental Engineering**	Spring semester, 2014 Restricted access
Writer: **Abdul Karim Farouk**	…… (Writer's signature)

Faculty supervisor: **Professor Torleiv Bilstad**

External supervisor(s): **Dr. Saeed Bikass**

Thesis title:

Study of the Process, Design and Operating Parameters Effect on the Efficiency of the Process Mill

Credits (ECTS): **30**

Key words: **Waste management, drill cuttings, thermal treatment, TCC, Process mill**	Pages: **66** Stavanger, **11th July/2014** Date/year

ABSTRACT

The study is dedicated to a computational model for the process mill using finite element software precisely COMSOL Multiphysics 4.4. A finite element model of the process mill was constructed using dimensions similar to the actual process mill. The model was simulated under the current operating conditions of the process mill and was referred to as the reference simulation in this work. This gave us the basis for comparing the various effects on the relevant parameters on the process mill. The simulation was extended to cover the effects of some selected design, process, and operating parameters on the velocity magnitude, the velocity profile as well as the effect on the efficiency of the process mill.

A major advancement in this regard was the different graphical display of results after computing the model with COMSOL multiphysics. The study of several parameters within affordable computational time was dependent on the mesh size.

Furthermore, an algorithm was developed in order to determine the response time of temperature change inside the process mill through a particular location in the simulation domain. The effect of relevant process parameters and the thermocouple tip position on the lag in temperature transmission was studied for models without liners and models with tungsten carbide liners.

The visualization of complete simulation data for each FE model was devised in Microsoft Excel.

The effect of viscosity, hammer thickness, angle between adjacent hammers, distance between adjacent hammers, rotational frequency and number of hammers on the velocity magnitude and the efficiency of the FE model of the process mill were also studied through simulations.

CONTENTS

ACKNOWLEDGEMENT

I thank the Almighty God for his guidance, protection, and the numerous favours which he has bestowed upon me.

It is difficult to mention everyone who contributed to the success of this project work. I will therefore express my appreciation to those who have been with me, influenced me positively and contributed to the development of my knowledge and personal skills.

I would like to express my sincere gratitude to Professor Torleiv Bilstad for being such a helping supervisor and arranging COMSOL Multiphysics software for me. Without his advice and unique guidance, this thesis would never have become a reality. I would like to express my appreciation to Evgenia Protasova, the assistant of Torleiv for her time, comments and dedication throughout the work.

I am thankful to Theodor Ivesdal the COMSOL administrator at UiS for providing me the COMSOL multiphysics software and access to the licence server throughout the work.

I am grateful to Dr. Saeed Bikass for his patience, for his wisdom, for being so present for me and for guiding me in using COMSOL Multiphysics. He has contributed immensely to the success of this project as my external supervisor.

I would like to thank Thermtec As and their entire staff for their kind gesture and for opening their doors for me to use their facilities. I do appreciate their contributions a lot.

I wouldn’t be able to come to study in Stavanger and to have such experience without the financial support of my Cousin Andrews Opoku-Agyemang. I owe him my sincere thanks.

Finally, I wish to express my thanks to my parents, who have supported me in every step of life. I am very grateful for the infinite love and care they have for me.

LIST OF FIGURES

LIST OF TABLES

LIST OF SYMBOLS

PART ONE: OVERVIEW

1 INTRODUCTION

In recent times, the demand for petroleum products has increased across the globe due to the increase in fuel and energy consumption. This has challenged the oil and gas producing companies to explore new fields in other to meet the market demand. Drilling of exploration and producing wells comes with a huge sum of drill cuttings contaminated with hydrocarbons (Quintero, 2003).

The contaminated cuttings pose environmental threat when released directly into the environment without any effective treatment. Different technologies with varying end-product quality are employed in the cuttings treatment industry due to the differences in the environmental regulations across the globe (Separation technology Hand-out, 2013)

Oil base mud cuttings present a complex and costly waste management challenge. The Thermomechanical Cuttings Cleaner (TCC) in combination with fluid recovery and reuse is recognized as one of the most effective means of drill cuttings treatment. The TCC converts the mechanical energy generated by the hammer mill into thermal energy to effect flash evaporation of the fluid to produce dry solids and recovered base oil of high quality and process water. The hydrocarbon content of the processed solids is very minimal (Kleppe, 2009).

Modelling the process mill using COMSOL multiphysics increased our knowledge on design and optimization of the process mill.

In addition, the temperature change response time inside the process mill was studied. This improved our understanding of what happens within the process mill, which led to suggestions on optimal design of the process mill in order to increase its efficiency.

An insight of the effect of some process parameters, design parameters and operating parameters on the efficiency of the process mill was investigated. This was done in order to improve the optimal operation of the process mill. Understanding the effect of these parameters will improve the design and performance of the process mill.

1.1 Main objective

The main objective of the project is to study the effect of some process parameters, design parameters and operating parameters on the efficiency of the process mill.

1.2 Specific Objectives

The specific objectives are the process we need to go through in order to achieve the main objectives and these are as follows:

i. To review the literature about mills
ii. To review the thermal cleaning of oily waste
iii. To learn finite element modelling and simulation
iv. To simulate models that describe the process mill using COMSOL Multiphysics
v. To analyse the response time of temperature change inside the process mill
vi. To study the effect of some process parameters, design parameters, and operating parameters on the velocity magnitude inside the process mill.

2 LITERATURE REVIEW

2.1 Equipment

2.1.1 Mills

Mill is a comminution device that breaks down mineral ore or particles into smaller pieces. Comminution involves all the size reduction processes. It may occur in one or several steps with techniques such as impact, compression or friction. The Figure 1 illustrates the different techniques of size reduction. Size reduction includes processes such as crushing, grinding, fine grinding, and ultra-fine grinding. The particle size can be reduced further into powdery form depending on the required product size. Grinding is achieved by the application of a mechanical force to the feed particles. Milling is achieved by a combination of impact and friction forces. The mechanical force breaks down the feed material to produce a finer product.

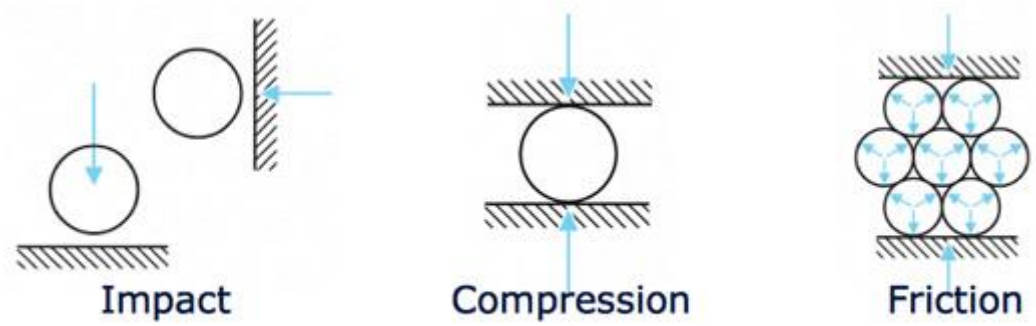

Figure 1 The different techniques of size reduction (Source: Magotteaux, 2010)

2.1.2 Mill Types and their Applications

Structurally, each type of mill consists of a horizontal cylindrical shell, provided with renewable wearing liners and a charge of grinding medium. The cylindrical shell is supported so as to rotate on its axis on hollow trunnions attached to the end walls (Gaudin, 1971).

Ball, rod and autogenous mills belong to a class of mills known as tumbling mills. Figure 2 shows a typical tumbling mill. Rod, ball and autogenous mills are similar in appearance and in general operating principle but differ in their grinding media. The grinding medium may be steel rods, balls or the ore itself.

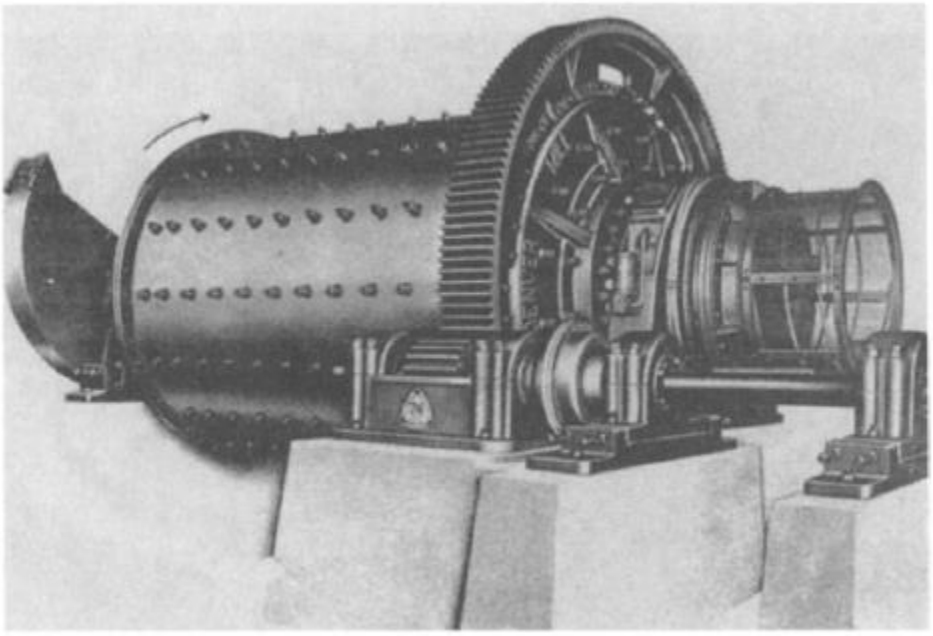

Figure 2 Tumbling mills. (Source: Wills, 2006)

2.1.3 Autogenous Mills

Autogenous mills comprise of two kinds, autogenous grinding mills (AG) and semi-autogenous grinding mills (SAG). An autogenous mill is a tumbling mill that utilizes ore itself as grinding media. Also, a semi-autogenous mill is an autogenous mill that utilizes steel balls in addition to the natural grinding media. Advantages of autogenous and semi-autogenous grinding mills are their lower capital cost, the ability to treat a wide range of ore type including sticky and clayey feeds, lower man power requirements and reduced grinding media expense (Wills, 2006).

2.1.4 Rod Mills

Rod mills may be considered as either course grinding or fine crushing machines. In a rod mill, steel rods extending the whole length of the mill are used as grinding media. This is shown in Figure 3. Rod mills deliver a more uniform fine product, but they are not suitable for very tough materials (Perry, 1997). Rod mills are particularly useful with sticky materials which hold balls together in aggregates (Coulson *et al*., 2002).

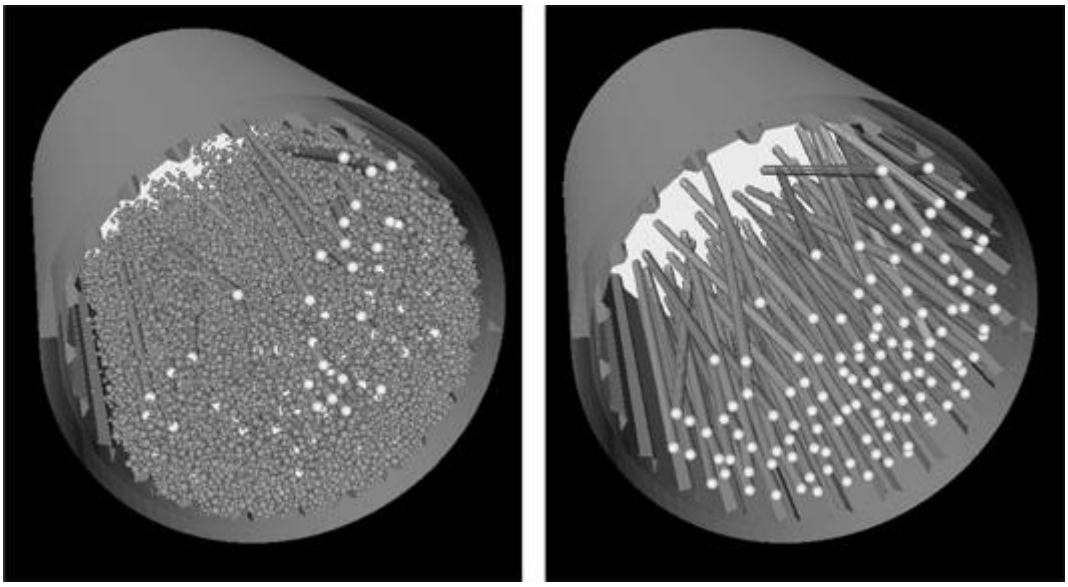

Figure 3 Rod mill filled with rods as the grinding media (Source: Magotteaux, 2010)

2.1.5 Vibratory Mills

The horizontal tube mill is the main form of industrial vibratory mill. It has two horizontal tubes that are mounted on springs. It is given a circular vibration by the rotation of a counterweight. Many feed flow arrangements are possible, adapting to various applications. Variations include polymer lining to prevent iron contamination, blending of several components, milling under inert gas and at high and low temperatures. The vertical vibratory mill has good wear values and a low-noise output. It has an unfavourable residence-time distribution, since in continuous operation it behaves like a well-stirred vessel (Perry, 1997).

2.1.6 Ball mills

Ball mills serve as a final stage in comminution. Ball mills may be classified according to the shape of the mill, method of discharging the ground ore, and whether the grinding is conducted dry or wet. Mills that fall under these classifications are tube mills, cylindroconical mills and cylindrical mills. A particular class of ball mill may be preferred depending on the nature of the feed and whether dry or wet grinding is required (Gaudin, 1971).

The material to be ground is fed in through a hollow trunnion at one end and the product leaves through a similar trunnion at the other end. During grinding, the balls which wear and are constantly replaced by new ones. This makes the mill to contain balls of various sizes. The outlet is covered with a coarse screen to prevent the escape of the balls. The inner surface of the cylinder is lined with an abrasion-resistant material such as rubber to decrease wearing (Coulson *et al*., 2002).

The rolling of the grinding media from top to bottom of the heap is called cascading. Cataracting is the throwing of the grinding media through the air to the toe of the heap (Perry, 1997). The balls will not fall away from the mill's shell at a certain rotational speed. This rotational speed is termed the critical speed of the mill. The Critical Speed, N_c of a mill is the rotational speed at which the centrifugal forces equal gravitational forces at the mill shell's inside surface (Sagmilling Inc., 2014). Mathematically the critical speed is defined by Perry (1997) as:

$$N_c = \frac{42.3}{\sqrt{D}}$$

Where
N_c = the critical speed, rpm (revolutions per minute)
D = the mill effective inside diameter, m

2.1.7 Tube Mills

Tube mill is the term applied to a mill of uniform diameter with greater ratio of length to diameter, in the range of 4 to 5 (Walas, 1990). The cylindrical section of the tube mill is divided into a number of compartments by vertical perforated plates. The material flows axially along the mill and can pass from one compartment to the next only when its size has been reduced to less than that of the perforations in the plate. Each compartment is supplied with balls of a different size. The large balls are at the entry end and thus operate on the feed material, whilst the small balls come into contact with the material immediately before it is discharged (Coulson *et al*., 2002). This results in the formation of a uniform product. It also gives an improved residence time distribution for the material (Perry, 1997). Figure 4 is a schematic of tube mill.

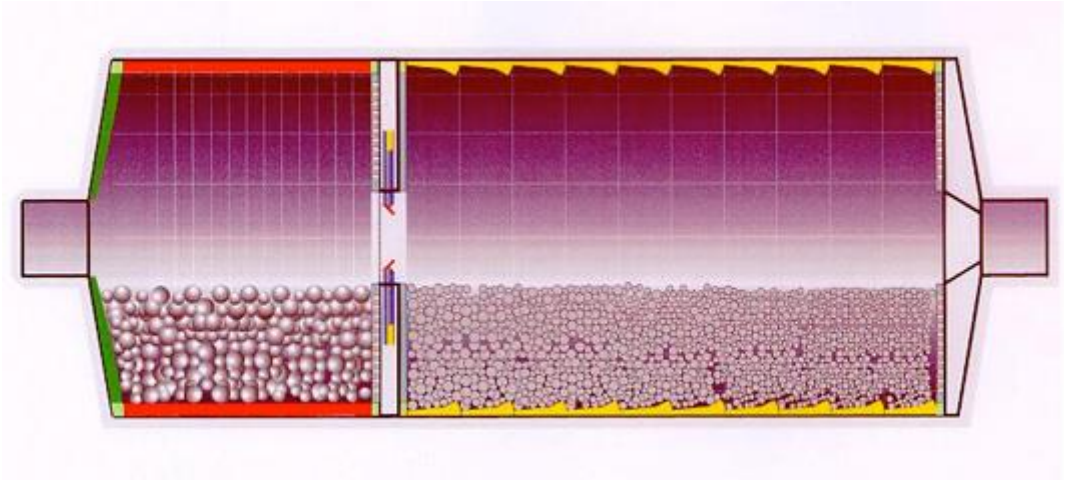

Figure 4 Schematic of tube mill charged with balls of different diameter (Magotteaux, 2010)

2.1.8 Cylindroconical Mills

The only significant representative of this class of mills is the hardinge mill. The hardinge mill consists of two conical sections connected by a short cylindrical section supported by end bearings on which hollow trunnions revolve. The conical section toward the feed end is obtuse, and that toward the discharge end is acute. The conical shape compels coarse particles and large balls to seek the cylindrical section of the mill, whereas fine particles and small balls are found in the conical sections. Advantages of the hardinge mill are the preferential grinding of coarse particles by large balls and of fine particles by small balls (Gaudin, 1971). Figure 5 shows a typical hardinge mill showing distributions of balls.

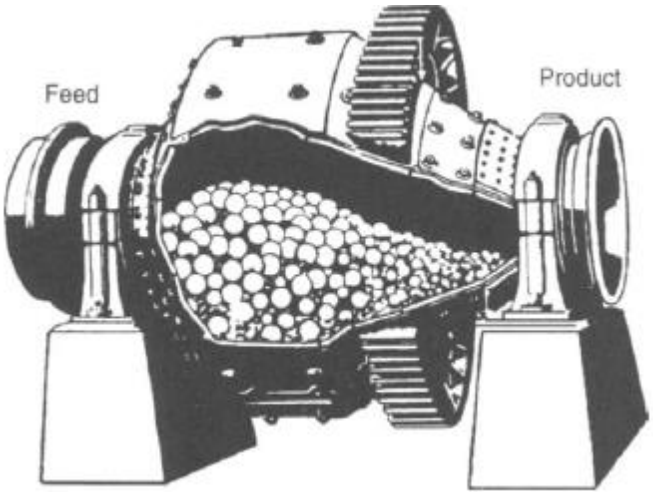

Figure 5 Hardinge Mill (Source: Wills, 2006).

2.1.9 Cylindrical Mills

Cylindrical mills are ball mills that possess a cylindrical shell. They are categorised based on the method employed in discharging the ground product. Peripheral discharge mill, trunnion overflow mills and grate discharge mills fall under this category. Product from the peripheral discharge mill is discharged through screens along the cylindrical shell. In the trunnion overflow mills, products are discharged by free overflow from the mill axis. The grate mill discharges product through a grate extending as a diaphragm across the full section of the mill near the discharge end. The Figure 6 is the schematic of different ball mill discharge design. The choice a particular discharge method for the ground product depends on the nature of the feed and whether dry or wet grinding is preferred (Gaudin, 1971).

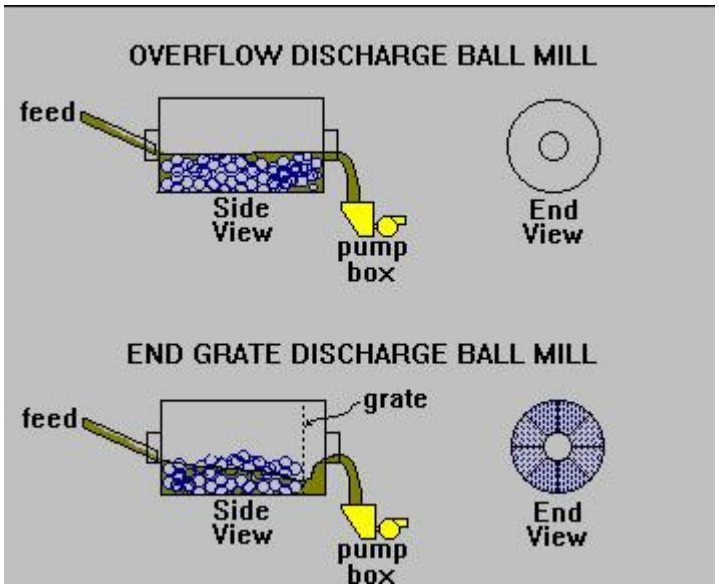

Figure 6 Schematic of different ball mill discharge design. (Source: John Meech, 2012)

2.1.10 Fitz mills

Fitz mill are high-speed screen hammer mills with flat hammers for impact. Sharp or narrow hammers are employed for milling tough plastic or fibrous materials. Figure 7 is an example of Fitz mill. Fitz mill are mostly used in the chemical, pharmaceutical and food processing industry (Fitzpatrick, 2014).

Figure 7 Fitz mill (Source: Fitzpatrick, 2014)

2.1.11 Hammer Mills

Hammer mill has swinging hammerheads which is attached to a rotor. The rotor rotates at high speed inside a stator during milling. This causes the feed material to crush and pulverize between the hammers and the stator. Hammer mills for fine pulverizing and disintegration are operated at high speeds. Generally, the rotor shaft is horizontal but can also be vertical. The shaft carries hammers, sometimes called beaters. The hammers may be T-shaped elements, stirrups or bars (NZIFST Inc., 1983). The hammers can be rings fixed to the shaft or to disks fixed to the shaft. The grinding action results from impact and attrition between lumps or particles of the material being ground, the stator, and the grinding elements. A cylindrical screen or grating usually encloses all or part of the rotor as shown in Figure 8 (Perry, 1997).

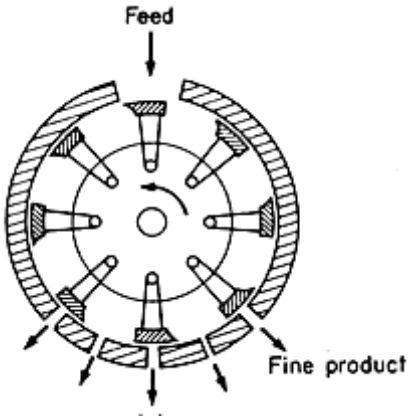

Figure 8 Schematic of hammer mill (Source:NZIFST Inc., 1983)

The fineness of product can be regulated by changing rotor speed, feed rate, or clearance between hammers and grinding plates. Changing the number and type of hammers used and the size of discharge openings improves product fineness. The feed must be nonabrasive with a hardness of 1.5 or less. The mill is capable of taking 2 cm feed material, depending on the size of the feed throat. The milled product can pass a No. 200 sieve (Perry, 1997).

Lumps or feed materials larger than 4 cm may be crushed with crushers before milling with hammer mills. The wear resistance of hammers can be improved with tungsten carbide or stellite tipping. Stellite is a group of cobalt-chromium alloy with high wear resistance (Kennametal satellite, 2013: Perry, 1997)

An air injector feeder can be supplied to project the feed particles directly in front of the hammer tips. This provides a more direct blow and thus increasing the mill efficiency. Wet feed can be charged with feed screws or pumps for wet grinding (Perry, 1997).

2.1.12 Hammer Mills with Internal Air Classifiers

Hammer mills with air classifiers are grinding elements comprising of classifier, fan and a hammer mill. They operate at high hammer-tip speed of about 7600 m/min. The high rotation speed of the hammers makes grinding effective. Figure 9 shows a schematic of hammer mill with internal air classifiers. The milled product is blown by an air stream into the discharge port. The fine product is separated by a cyclone collector into a suitable container (Perry, 1997).

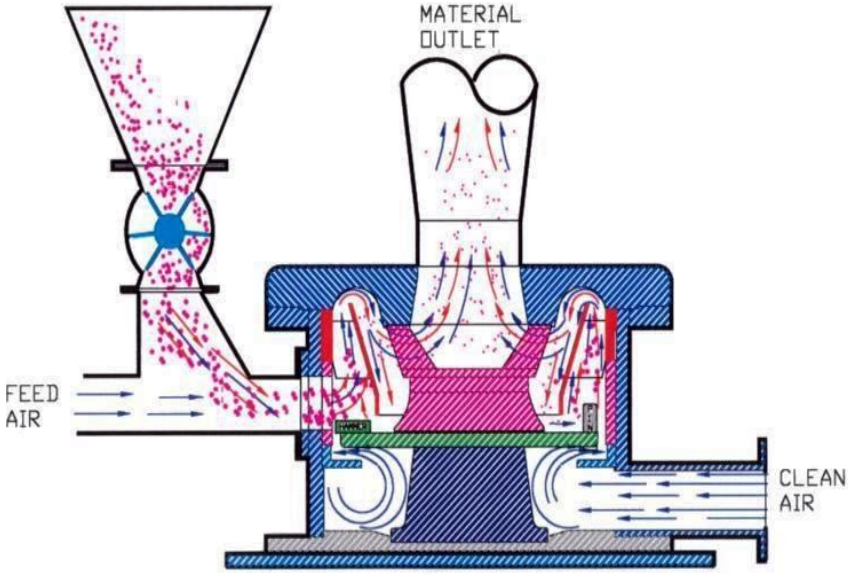

Figure 9 Schematic of hammer mill with air classifier (Source: Classifier Milling Systems Inc, 2010)

2.1.13 Jeffrey Hammer Mills

Jeffrey hammer mill have rectangular swing hammers or rigid hammers. The choice of hammer type depends on the application of the mill. Rigid hammers are used in slow speed application such as shredding of waste paper, fibreglass mats or rubber. Rectangular swing hammers are used for grinding friable materials such as limestone.

Jeffrey hammer mill may be design with or without screen grates. Figure 10 shows a Jeffrey hammer mill with screen grate and its longitudinal section. The screen grates have capacities ranging from 50 to 140 ton/h for a product with top size 45 mm. The rotational speed of the hammers varies between 500 and 1800 rpm (Jeffrey Rader, 2014)

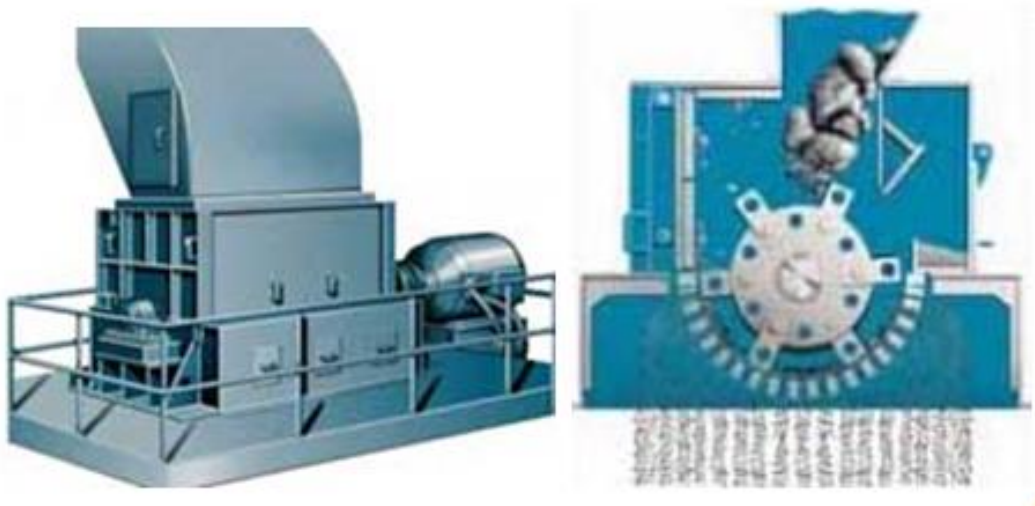

Figure 10 Jeffery hammer mill and its longitudinal section (Source: Jeffrey Rader, 2014)

2.1.14 Rotor Impactors

The rotor comprises of a tough steel bar attached to a cylinder. This is mounted in a rotating drum to form the rotor impactor. Its mode of operation is by impact breaking. There is a high collision speed between the rock material, the moving and the stationary bars inside the machine are high. This causes rock on rock collisions which contributes to size reduction. Figure 11 is an example of the GSK-type rotor.

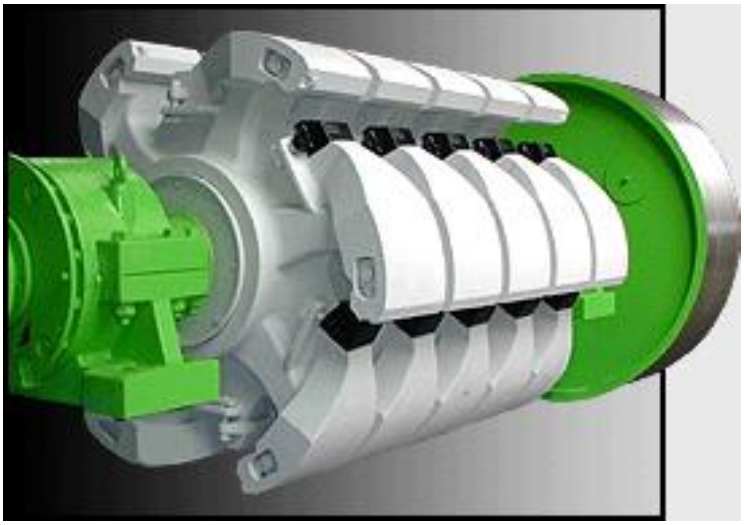

Figure 11 GSK-Type rotor (Source: Hazemag Inc., 2014)

Rotor impactors are best use for crushing wet or sticky clays, shale and other similar materials. It is efficient in milling wet and sticky materials to finer products. This results in a higher reduction ratio. Usually, there is no secondary and tertiary crushing stage due to the high reduction ratio (RQI Inc., 2010).

2.2 Control of Grinding Circuits

Processing plants requires constant supervision and control for smooth operation. Process control is done to increase the plant output. The required product specification is produced by adequate process control (Perry, 1997).

Industrial control systems could be feedback or feed forward control loops. Process parameters are measured with measuring devices. For example temperature is measured with thermocouple. They are controlled from deviating from the set point in order to achieve smooth operation (Coulson *et al*., 2002). The performance of process plants can be increased by 2 – 10% by the installation of single-variable automatic controls.

In practical situations, process parameters are not always static. They keep varying during plant operation. Controlling the plant circuit in a timely manner so that it operates close to its optimum state is termed optimal control. The optimum state varies as the feed conditions and operating parameters change (Perry, 1997).

2.2.1 Motor and Drive

One of the basic ideas of process economics is to minimize cost and maximize profit. Equipment are designed or specified in a cost effective manner. Motors should be specified such that it has a lower operating cost. The motor must have high availability and low

maintenance down time. Rolling mills are one of the most demanding applications for motor drives. Each rolling stand consists of a top and a bottom roll. They are driven through a gearbox by an electric motor. A typical motor size for modern mills is 600 kW to 1200 kW for each stand. The motor drives are controlled by a loop control system. (RUSSULA IE&S group, 2013)

The ring motor is a low-frequency concurrent motor. Its windings are mounted directly on the mill shell. The ring motor has higher initial cost but the operating cost is lower. The downtime for maintenance is lower. The availability is about 99% according to Perry (1997).

2.2.2 Energy Laws

Comminution equipment use energy to achieve the required product size. The laws of comminution describe the relationship between the energy consumed by the comminution device and the degree of size reduction achieved. The efficiency of the energy utilization and the size distribution is dependent on the mode of comminution and the specific comminution device employed. The mode of comminution can be abrasion, impact or shear. The energy required to mill material was suggested by Austin (1964) to be inversely correlated to the particle size of the product. This can be express as;

$$E \propto (P_{80})^{-n}$$

Where

E = the energy required for the comminution process

P_{80} = particle size at which 80% of the material will pass when screened

n = exponent characteristic of the comminution device, product size range, and material

Figure 12 represent the energy requirement for comminution as determined by Hukki (1975). It illustrates the range of applicability of Rittinger's, Bond's and Kick's law as indicated by the different applicable values for the exponent in the equation $E= K (P_{80})^{-n}$

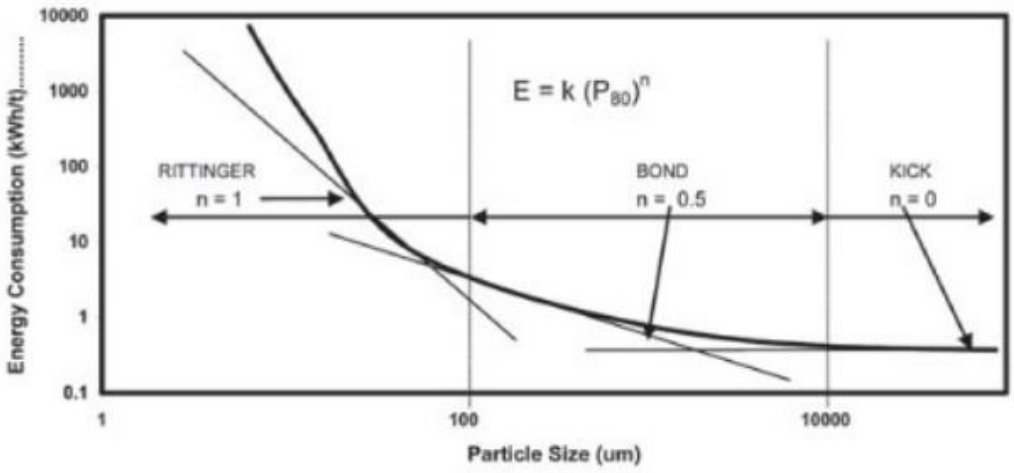

Figure 12 The energy requirement for comminution as determined by Hukki (1975). (Source:The Southern African Institute of Mining and Metallurgy, 2014)

Kick proposed that the energy needed to crush a solid material to a specified fraction of its original size is the same, regardless of the original size of the feed material (NZIFST Inc., 1983).

Rittinger proposed that the energy required for comminution is proportional to the new surface produced (Perry, 1997). The representation of Rittinger's laws on Figure 12 is a point. This point has been approximated over a wider range of product sizes (Southern African Institute of Mining and Metallurgy, 2014)
Generally, the differential equation defining the energy laws is given as:

$$dE = -C\frac{dX}{Xn} \qquad \text{(Perry 1997)}$$

Where
E = the work done,
X = the particle size,
C, n = constant
The solution to this differential equation is the Kick's, Rittinger's or Bond's law. The Kick's law can be written as:

$$E = C\log\left(\frac{X_F}{X_P}\right) \qquad \text{(Perry, 1997)}$$

Where
C = Kick's constant
X_F = the feed-particle size,
X_P = the product size,
X_F /X_P = the reduction ratio.
The Rittinger's law can be written as:

$$\mathrm{E} = \left(\frac{\mathrm{C}}{\mathrm{n}-1}\right)\left(\frac{1}{\mathrm{X_p^n}-1} - \frac{1}{\mathrm{X_F^n}-1}\right) \qquad \text{(Perry, 1997)}$$

Where
C = Rittinger's constant
X_F = the feed-particle size,
X_P = the product size,

The Bond law can be written as:

$$\mathrm{E} = 100\mathrm{E_i}\left(\frac{1}{\sqrt{\mathrm{X_p}}} - \frac{1}{\sqrt{\mathrm{X_F}}}\right) \qquad \text{(Perry, 1997)}$$

Where
E_i = the Bond work index**.** The Bond work index is the work required to reduce unit mass of the material from an infinitely large feed size to such a size that 80% of the product passes a 100-µm screen (Southern African Institute of Mining and Metallurgy, 2014: Perry, 1997)

2.2.3 Grinding Efficiency

According to the Coalition for Eco-Efficient Comminution (CEEC), comminution consumes about 3% of the world electrical energy. Most of the energy is dissipated to the milled product as heat. The equipment and the surrounding atmosphere gain some of this energy as heat. The energy efficiency of a grinding operation is the energy consumed compared with some ideal energy requirement. The efficiency of the grinding mill can be increased by decreasing the feed size upstream of the mill. The feed size can reduce by crushing with crushers prior to milling. (CEEC, 2012: Natural Resources Canada, 2014)

2.3 Safety

Grinding media may be hazardous due to their flammability. Metal powders and non-metallic are potential fire hazard during grinding. This is due to the flammability limits and high grinding temperature. Examples of such non-metallic are sulphur, starch, wood flour, cereal dust, dextrin, coal, pitch, hard rubber and plastics. Fires or explosion may be initiated by electric sparks, hot surfaces, and spontaneous combustion during operation (Perry, 1997).

Toxic, bio-reactive or radioactive feed material must be handled carefully during milling. They should be isolated and their exposure minimised to promote safety.

Combustible dust is any fine material that can ignite when suspended in air. Ignition of combustible dust can result in a flash fire or explosion. The particle size and concentration of dust in air determines the level of explosion. Finer particles ignite easily and the rate of combustion is rapid (Fire inspection and prevention initiative, 2014). Explosion cannot occur below the lower flammability limit (LFL) of the material. The lower flammability limit is the minimum concentration in air below which propagation of flame does not occur on contact with an ignition source. This is because the heat of combustion is not enough to cause explosion. Explosion cannot occur above the upper flammability limit (UFL) of the material. The upper flammability limit is the maximum concentration in air above which propagation of flame does not occur. This is due to the presence of insufficient oxygen to initiate combustion. Figure 13 shows the dependency of explosion pressure on concentration of vapour/gas in air (OSHA, 2013; Perry, 1997)

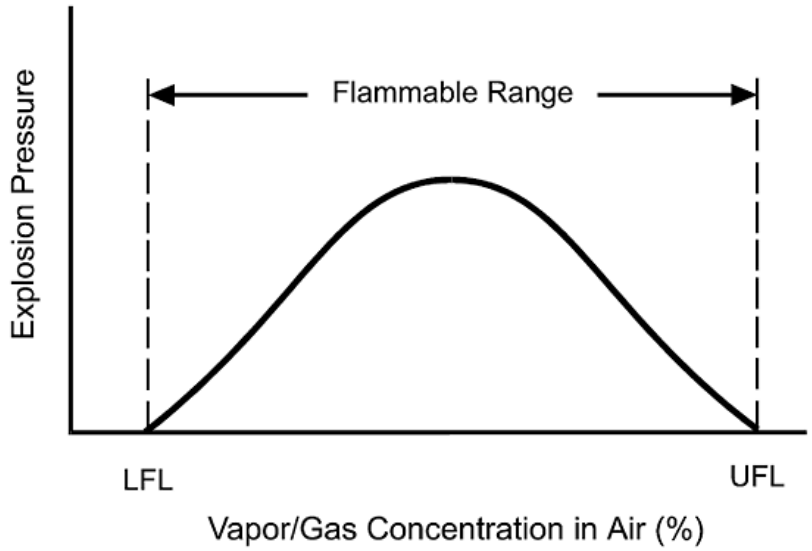

Figure 13 Explosion pressure as a function of material concentration in air (Source: OSHA, 2013)

Safety precautions must be taken during the design phase. Materials with less sparking tendency such as steel should be used in building the mill. Magnetic separators can be used to take out foreign magnetic material from the feed. This is a useful precaution during plant operation (Perry, 1997). Table 1 shows the minimum autoignition temperature, AIT of some combustible gases and liquids in air and oxygen at 1 atm.

Table 1 Minimum Autoignition temperature, AIT of combustible gases and liquids in air and oxygen at 1 atm (Source: Kuchta, 1985)

Combustibles	Minimum Autoignition Temperatures AIT, ^{o}C	
	Air	**Oxygen**
Methane	630	555
Ethane	515	505
Propane	450	NA
n-Butane	370	285
Isobutane	460	320
n-pentane	260	260
n-Hexane	225	220
n-Heptane	225	210
n-Octane	220	210
n-Decane	210	200
Acetylene	305	295
Ethylene	490	485
Propylene	460	425
Cyclopropane	500	455
Gasoline (100/130)	440	315
Kerosene	230	215

NA = Not available

The fraction of oxygen in air should be controlled during grinding. Low oxygen level in grinding systems aids in preventing dust explosions in equipment (Perry, 1997). Oxygen content below 12% is safe for grinding most materials, but 8 % is recommended for sulphur grinding. Grinding equipment is filled with inert gas. This is done in order to minimize the level of oxygen in the equipment. Flue gas is an alternative for inert gas. It mixes with the air present in a system. Comminution equipment should be provided with explosion vents (Perry, 1997).Table 2 shows the flammability limits of some combustible vapours in air and oxygen at 25^{o}C and 1 atm.

Table 2 Limits of flammability of combustible vapours in air and oxygen at 25°C and 1 atm (Source: Kuchta, 1985)

combustible	Flammability limits (volume %)			
	Air		Oxygen	
	LFL	UFL	LFL	UFL
Methane	5	15	5	61
Ethane	3	12.4	3	66
Propane	2.1	9.5	2.3	55
n-Butane	1.8	8.4	1.8	49
n-Hexane	1.2	7.4	1.2	52
n-Heptane	1.1	6.7	0.9	47
Acetylene	2.5	100	<2.5	100
Ethylene	2.7	36	2.9	80
Propylene	2.4	11	2.1	53
Cyclopropane	2.4	10.4	2.5	60
Benzene	1.3	7.9	<1.3	NA

NA = Not available

2.4 Wear and Wear rate control

Wearing is the erosion of materials in contact due to the mechanical action between them. The three main wear mechanisms are abrasion, impact and corrosion (Microtribodynamics Lab., 2004: Magotteaux, 2010) Figure 14 shows an example of wear as a result of these mechanisms.

Figure 14 Wearing of some mill components such as balls and liners as a result abrasion, corrosion and impact (Source: Magotteaux, 2010)

Grinding to produce finer products increases the wear rate of the mill components. High energy input is required to produce finer product (Microtribodynamics Lab., 2004)

Mill wear rate is dependent on the hardness of the feed material, presence of corrosive minerals, and the feed particle size. The properties of the material of construction of the mill contribute to the wear rate. Environmental factor such as the pH, oxygen potential, and temperature may affect the mill wear rate (Perry, 1997).

Hardening the components surface decreases the wear rate. This is achieved by welding. Hardening improves maintenance and lower downtime. Wear rate is higher in wet grinding. Abrasion during grinding causes the removal of the protective oxide films. This increases the corrosion rate of the mill components (Perry, 1997).

The corrosion rate can be reduced by increasing the pH of the feed material. The component wear rate can be controlled by the use of wear resistance materials. This includes abrasion-resistant steels, alloyed cast irons, and non-metallic.
Chromium or molybdenum or a lower manganese grade (6 – 7%) can be used to improve the wear resistance of the mill components. This can increase the wear resistance of jaw-crusher elements. Hardening with chromium increases the wear resistance of gyratory cone-crusher mantles and hammer-mill parts.
Low-alloy steels are used for ball mill liners and grinding balls. Alloys containing nickel (4%) and chromium (2%) is a good wear resistance alloy. They are use as secondary mill liners.

High-chromium cast irons contain chromium (12 – 30%) and carbon (1.5 – 3.5%). Molybdenum and nickel may be added as secondary constituents. High–chromium cast iron is use to build components for tertiary dry-grinding applications (Perry, 1997).
Elimination of austenite in the structure can improve resistance to spalling. Spalling is the process that occurs when flakes are separated from a larger body of material. This is caused by corrosion, continual friction, or a direct impact with another objects (Wise Geek, 2014). Alloys with hardness between 52 - 65 Rockwell have a good wear resistance. Alloys with good wear resistance reduce the maintenance cost of equipment (Coulson *et al*., 2002; Perry, 1997).
Rubber and ceramics materials are also use as mill liner. Rubber has high resilience and good wear-resistant in low-impact abrasion. It is inert to corrosive wear. Rubber liners reduce noise during operation. Rubber is vulnerable to cutting abrasion. This causes the wear rate to increase when milling heavy particles. Rubber can swell and soften in solvents. Their installation is relatively easy due to its low density (Perry, 1997).
Ceramics liners can be used in place of metallic liners. This is done in situations where metallic contamination of product is not acceptable. Ceramics are used for milling cements and pigments. Roller mills and cyclones can be lined with ceramic tiles (Perry, 1997). Some processing equipment may be lined with ceramic. These include equipment for food processing, mineral processing, chemical processing, petrochemical plants, pulp and paper mills (CoorsTek Inc., 2014).

The hammer mill can be considered as the best mill type for the TCC process. This is because the hammer mill can handle a variety of feed types ranging from sticky clay to shale in an efficient manner to finer products. This is of no exception to drill cuttings which is a mixture of hydrocarbons, water, sand, rocks particles and clay.
Using the hammer mill in the TCC process presents a couple of advantages over the other mill types. The hammer mill's ability to produce ultrafine products tends to increase the surface area of the drill cuttings being treated in the TCC. The increase in surface area helps to increase the rate of evaporation of water and hydrocarbons from the drill cuttings being processed.
During processing, the TCC uses the energy that will be dissipated by the hammer mill to the milled product as the heating source to evaporate the water and hydrocarbons content of the drill cuttings in other to produce dry solids free of hydrocarbons. This is an efficient way of using the dissipated heat there by making the TCC process more energy efficient.

3 TREATING OF OILY WASTES

Drill cuttings are produced due to the drilling of explored wells, production wells, and injection wells in the geological formation. Drill cuttings are usually contaminated with drilling mud, dissolved salts, heavy metals and trace amounts of radioactive elements. This is a hazardous waste that needs to be treated to remove the hydrocarbons and other toxic chemicals that might have adverse effect on the biotic environment, before discharging into the environment (Kleppe, 2009; Quintero, 2003; Separation technology Handout, 2013).

The differences in environmental regulations across the globe have led to the development of different technologies with different end-product quality in the cuttings treatment industry. The various ways for drilling waste management includes, waste minimization, oxidatively incinerating oil, disposal at remote site, re-circulation of the drilling mud, drill cuttings re-injection (DCRI), (Quintero, 2003), bioremediation, thermal desorption (Kleppe, 2009) and cleaning with surfactant. In situations where the treated cuttings will be discharged into marine environment, the chosen treatment method should be able to make the cuttings water wet-able (Quintero, 2003). The Figure 15 shows the various approaches in environmental management of drilling waste.

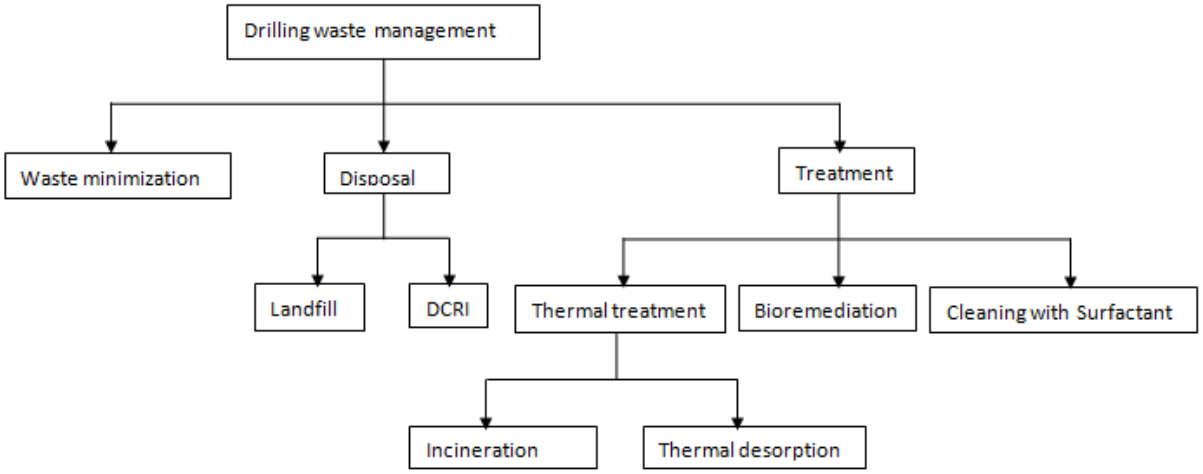

Figure 15 Different techniques used for drilling waste management

3.1 Waste minimization

Drilling waste minimization can be achieved by following good drilling practices such as directional drilling, drilling by coiled-tubing and pneumatic drilling. Such drilling practices will minimize the rate of drilling waste generation as the drilling mud is utilised efficiently.

3.2 Recirculation of the drilling mud

Drilling mud is recirculated throughout the drilling process. As the drilling mud rises to the surface, it passes through screens which trap the drill cuttings from the borehole, before being cycled back into the system which delivers mud to the head of the drill bit. This recirculation process is designed to cut down on waste by reusing as much mud as possible. The process includes a preliminary separator (shale shakers) which separates the cuttings from the mud before it is recirculated as show in Figure 16 (Morris, 1981; PISZCZ et al., 2009; Quintero and Limia, 2003; Sample Jr, 1979; Petrolyte, 2011).

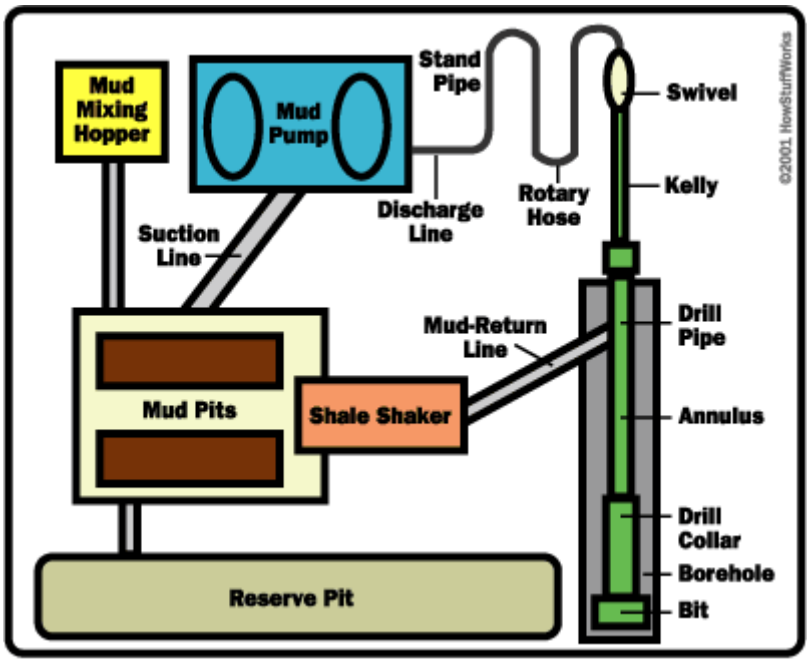

Figure 16 Recirculation of drilling mud. During recirculation, the drill cuttings passes through screens which trap the materials from the well, before being cycled back into the system which delivers mud to the head of the drill bit (Source: Petrolyte, 2011)

3.3 Disposal

Cuttings disposal at remote sites is cheap and practised where there are flexible environmental regulations. Direct disposal is relatively cheap but transportation is expensive and there is a higher risk of environmental pollution during transportation (Morris, 1981). Cuttings may be disposed off in landfills without prior treatment in regions with flexible environmental regulations. Handling this hazardous waste i.e. loading and offloading poses health threat to workers.

3.4 Drill Cuttings Re-injection (DCRI)

Re-injection of oil-contaminated drill cuttings is attracting considerable attention as a cost-effective means of complying with environmental legislation concerning discharges of drilling waste (Guo, 2007; Hagan, 2002; Quintero, 2003). However it means high consumption of energy and contributes to CO_2 pollution when diesel driven pumps are used

The drill cuttings are processed into slurry by grinding it into smaller particles and mixing with water. The slurry is then injected into an underground formation at high pressure enough to fracture geological formations (Separation technology Handout, 2013)

Annular injection and injection into dedicated well are the two common types of drill cuttings injection. Annular injection involves introducing the slurry through the space between tow casing strings. When the slurry is injected into a section of the drilled hole that is below all casing strings it is termed dedicated well injection. Injecting slurry into a section of the casing that has been perforated with a series of holes at the depth of an injection is also known as dedicated well injection (Argonne, 2003). Figure 17 is a schematic of annular injection and dedicated well injection.

Drill cuttings injections must be preceded after geological considerations such as the permeability characteristics of the rock, rock fracture rate, size and configuration of fracture, drinking water aquifers. The common problems associated with drill cuttings injection includes plugging of the casing or piping with solids, erosion of casing, tubing and other system. Injection of drill cuttings may pose environmental problems as leakage into the environment (Separation technology Handout, 2013).

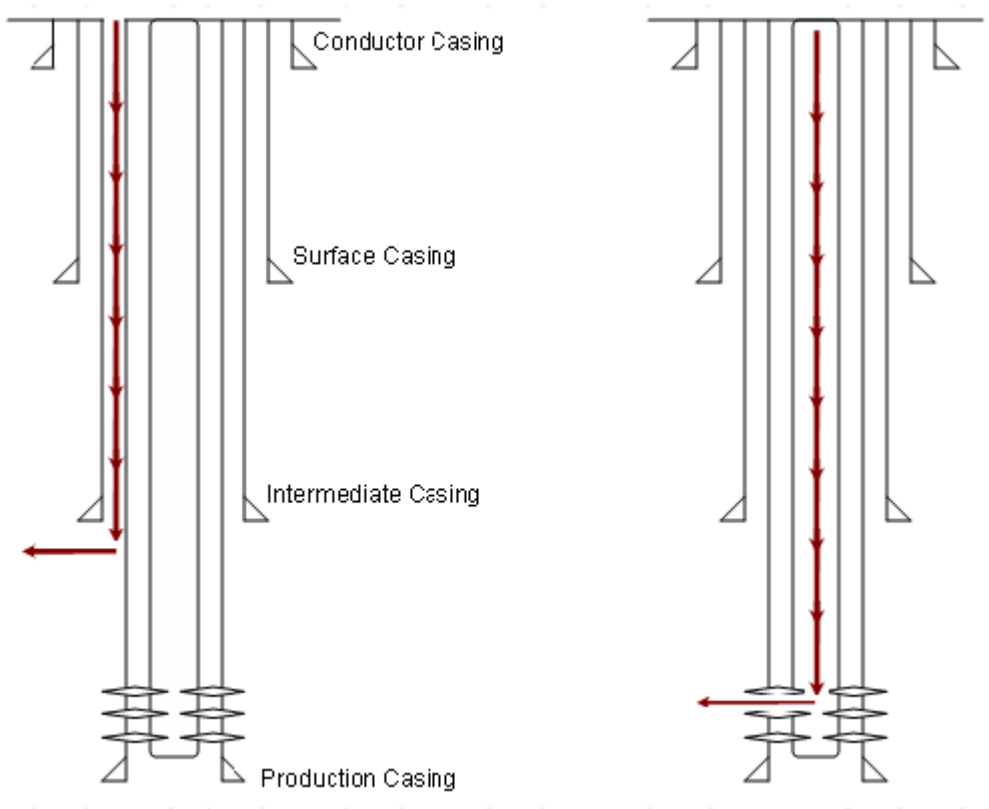

Figure 17 The two types of drill cuttings injection. Annulus injection (left) and dedicated well (right) as illustrated by Shadizadeh *et al*., 2012.

3.5 Cleaning of drill cuttings using surfactants

Drill cuttings can be cleaned by the addition of excess base oil to the cuttings and passing them through two stages of centrifuge. The solids are washed with aqueous surfactants, and then passed over shakers through a decanting centrifuge and into a three phase separator. The washed solution is then recycled and used to clean more cuttings. Cleaning of OBM cuttings with surfactants is illustrated in Figure 18 (Thomas *et al*., 2007).

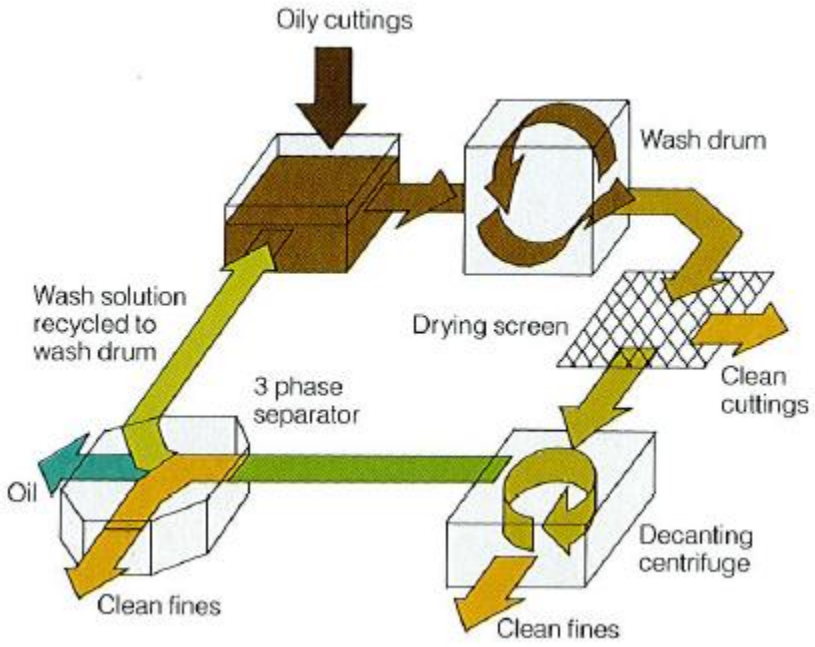

Figure 18 Cleaning of OBM cuttings with surfactants plus wash drum. Solids are washed in the aqueous surfactants, and then passed through three stages to separate liquid from fines which can be dumped (Thomas *et al*., 2007)

3.6 Bioremediation

Bioremediation of drill cuttings is the use of naturally occurring micro-organisms (yeast, fungi or bacteria) to break down and degrade organic substances present in the drill cuttings. The microorganisms break down the organic substances into carbon dioxide and water which is not harmful to the environment. The micro-organism population will reduce naturally after the contaminants are degraded. Figure 19 is an illustration of biodegradation of drill cuttings under controlled temperature and PH.

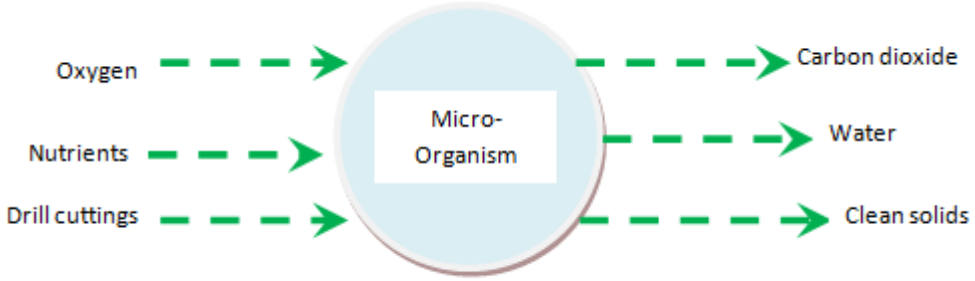

Figure 19 Bioremediation of drill cuttings showing the inputs and output of the process under controlled temperature and pH as described by Scomi-group 2008

This is because after the degradation of the hydrocarbons, there will be no source of food for the microbes. Bioremediation is relatively inexpensive compared to the other treatment methods. The products of bioremediation can be disposed off without further treatment at oil content less than 1 % w/w. The shortfall of this treatment method is that, the hydrocarbon that is degraded can be recovered by other treatment methods for re use. There is a high level of CO_2 pollution associated with biodegradation. The Figure 20 shows that the time taken to

degrade the hydrocarbon is dependent on the formation drilled the local soil and the type of oil base drilling fluid (Scomi-group, 2008).

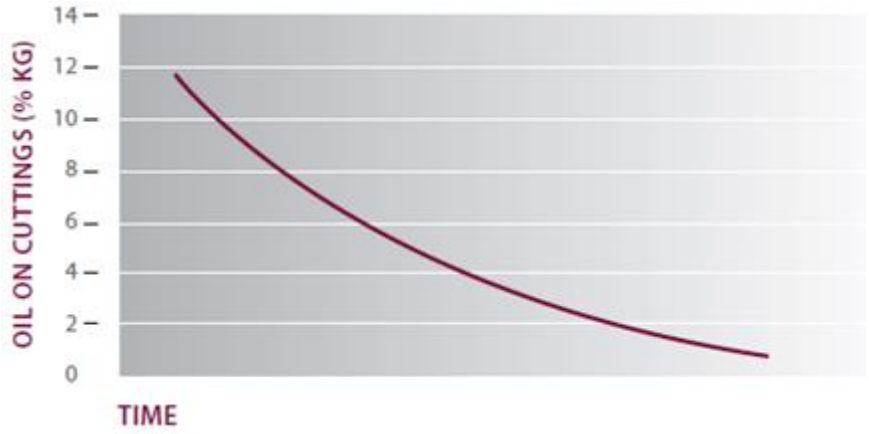

Figure 20 The time dependency of oil reduction due to micro-organism activities (Source: Scomi-group, 2008)

4 THERMAL CLEANING OF OILY WASTES

Thermal treatment is the use of high temperatures to recover or destroy hydrocarbon from hydrocarbon contaminated materials. Thermal treatment is suitable for treating the organic components of drill cuttings; however it may also reduce the volume and mobility of inorganic such as metals and salts (Bansal, K.M, and Sugiarto, 1991).

Further treatment may be required for metals and salts depending on the final fate of the wastes. Incineration and Thermal Desorption are the two categories of thermal treatment technologies.

4.1 Incineration

Incineration is the thermal oxidation of hazardous waste materials. The drill cuttings are combusted at high temperatures (1,200 ^{o}C–1,500 ^{o}C) to give non-hazardous pollution free cuttings. Incineration of drilling wastes occurs in rotary kilns, which incinerate any waste regardless of size and composition.

Incinerators are designed to burn off the organic components of oily waste by converting it to carbon dioxide and water vapour. Incineration of hazardous waste reduces the volume of waste and the amount of toxic compounds released into to the environment (La Crega et. al., 1994)

The inorganic components of the waste will remain in the incinerator ash. Metals such as arsenic, cadmium and mercury which may have a boiling point lower than the incinerator temperature may create problems in the flue gas. Incineration is not a good remedy for hazardous organic waste with high metallic content. However, appropriate air pollution control equipment can be installed to remove metals to acceptable flue gas levels prior to discharge into the atmosphere (La Crega et. al., 1994).

The product from an incinerator must be tested for unburned pollutants before disposal even though it gives good quality product at sufficient temperatures. Incineration comes with a high risk of explosion. It is associated with high air pollution due to high levels of CO_2, NO_x, and dioxins emissions (Kleppe, 2009; Morris, 1981; Sample Jr, 1979; Zupan, 2000).

4.2 Thermal desorption

The main principles of thermal desorption are steam stripping and non-oxidative thermal distillation to eliminate hydrocarbons and water from the drill cuttings. Treatment efficiency is related to the volatility of the contaminants. Thus light hydrocarbons, aromatics and other volatile organics are removed at low temperatures between 250 ^{o}C and 350 ^{o}C. Heavier compounds such as polycyclic aromatic hydrocarbons are less easily removed except for high temperature systems up to 520 ^{o}C (La Crega et. al., 1994). The products are solids, water condensates and oil condensates. It produces solids free of hydrocarbons that can be disposed off. The liquids are separated and reused in drilling mud to improve the economics of this method. The hydrocarbon condensed during the process can be reused as fuel to the burners (Quintero and Limia, 2003). Process temperatures above 400 ^{o}C may degrade the recovered hydrocarbons (Kleppe, 2009). The process is very effective and has a reduce risk to explosion and fire if the heating drum is operated under vacuum conditions. This is achieved by purging with N_2, CO_2 or any non-oxide gas degraded (El-sayed and Kamal H, 2001).

4.2.1 Thermomechanical Cuttings Cleaner (TCC) Technology

The thermomechanical cleaning of drill cuttings is achieved in the TCC as the kinetic energy from the rotating arms of the hammer mill is converted to thermal energy. Thus the friction between the cuttings and the hammer arms generates the thermal energy in the processing unit. The energy generated is high enough to evaporate the hydrocarbons and the liquid. The discharged solids are dry and pollution free. The hottest spot in the process is in the cuttings. The fluid flash evaporates and is under influence of the process temperature for only a few seconds. The Figure 21 is the principal sketch for the TCC (Kleppe, 2009).

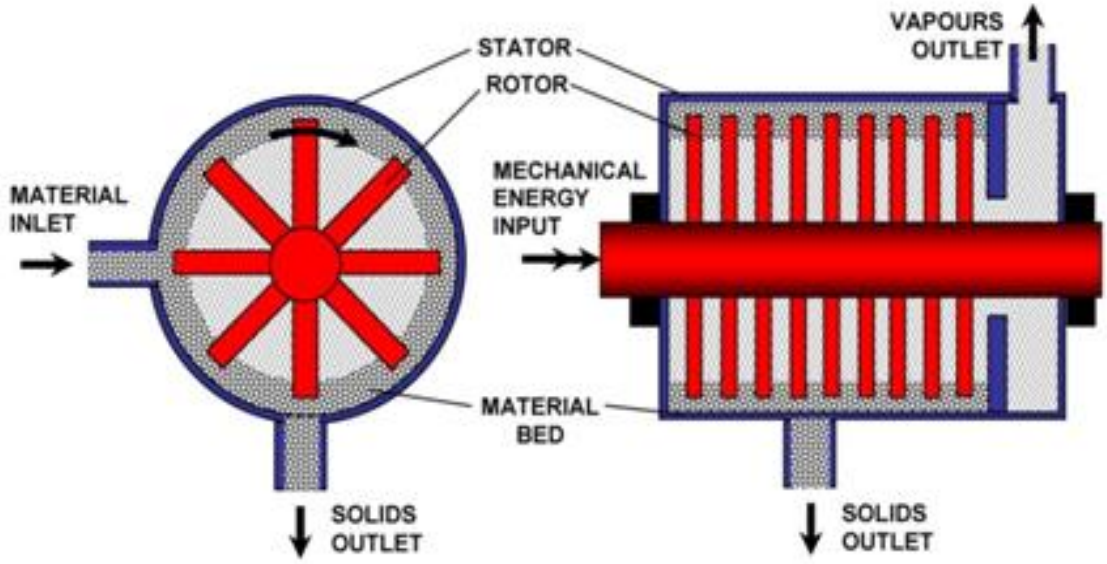

Figure 21 Principle sketch for TCC (Source: Thermtech, 2009)

A benefit of the TCC process is the intense agitation that efficiently breaks up the solid particles. This provides minimal diffusion distances for oils, which must overcome the capillary forces which bind the oil internally in the solid particles. From an environmental standpoint the advantage of the TCC thermo mechanical desorption process is the high degree of recovery of the hydrocarbons for reuse. Operators of the process are able to recover base oil for reuse in new drilling fluid, while the quality of the solid particles makes them potentially valuable as a filler material in different industrial products (Bilstad, 2013).

4.2.2 Unit Operations on the TCC Plant

The TCC plant includes such necessary units as: the process mill, vapour separation and oil water separation. The Figure 22 is schematic depicting of the TCC operations unit.

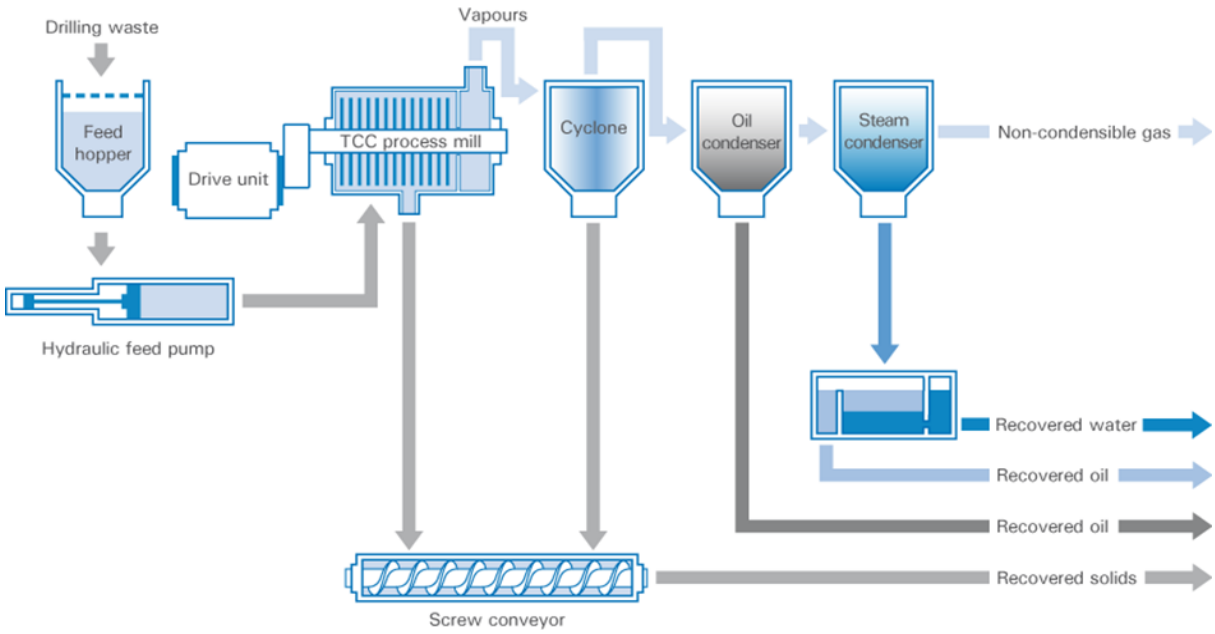

Figure 22 TCC schematic (Source: Thermtech, 2013)

4.2.3 The process mill

The process mill is a unit of the TCC treatment, where the mechanical energy supplied to the cuttings by the rotor (see Figure 21), is converted into thermal energy to facilitate the separation process. Feeding of the process mill is limited to 200-400 kg with a corresponding retention time of 6 -12 minutes for solids and 15 – 30 seconds for the oil. The process temperature is between 200 – 300 ^{o}C, which does not cause the oil to degrade (Bilstad, 2013; Thermtech, 2010).

The TCC is the only friction based thermal separation technology, which recovers for re-use the different components of the oily waste. Flash point changes of <2 ^{o}C of the recovered base oil compared to the virgin oil indicates that little or no cracking of the synthetic oil occurs in the process (Bilstad, 2013; Thermtech 2010). Kleppe, (2009) states that, ‘‘the energy balance for one metric ton per hour of cuttings with o/w/s of 15/15/70 is, if treated at 275°C and taken from a 20°C storage temperature, yields a power of 200 kW”.

4.2.4 Vapour separation

The vapour that flashes out of the process mill is condensed in the vapour separation unit to recover oil, water and some amount of solids. Traces of solids in the vapour are recovered by the cyclone, oil condenser recovers the oil and the steam condenser condenses the stem. The condensate is channelled to the oil water separator as in Figure 22 (Thermtech, 2013).

4.2.5 Oil water separator

Oil-water separator uses gravity separation to recover the oil and water in the steam condensate.

4.2.6 Product Quality

The composition of drilling fluids is different for different geological formation as well as the drill cuttings. This will therefore give products of different compositions, but expectations can be defined based on historical data from similar feedstock and similar operations (Thermtech, 2013).

4.2.7 Processed Solids

Thermtech (cited in Bilstad, 2013) explains that the solid phase from the TCC process is a light and dusty mineral powder with particle size in the range from 0.1 to 300 micrometers. The solids leaving the unit are hot and dry, appearing very lightweight and dusty. In most cases the powder is damped with the recovered water to avoid dusting. The bulk weight is typically 2 kg/dm^3. The solids carry a minor amount of organic matters and hydrocarbons, less than 4000 ppm.

4.2.8 Recovered oil

Thermtech (cited in Bilstad, 2013) states that, the base oils used for drilling fluids are well defined, low sulphur, low aromatics oils within the diesel range of distillation. Among the quality specifications for the base oil are density and flash point. In addition HSE requirements are low in aromatics, BTEX and sulphur. The Figure 23 and Figure 24 shows a sample GC – MS (gas chromatography - mass spectrometry) profile of used base oil before it is treated and base oil recovered in the hammer mill. The recovered oil is directly re-usable as base oil in new mud. The recovered oil is cleaned in several stages before it is discharged in two different fractions; the main fraction comes directly from the oil.

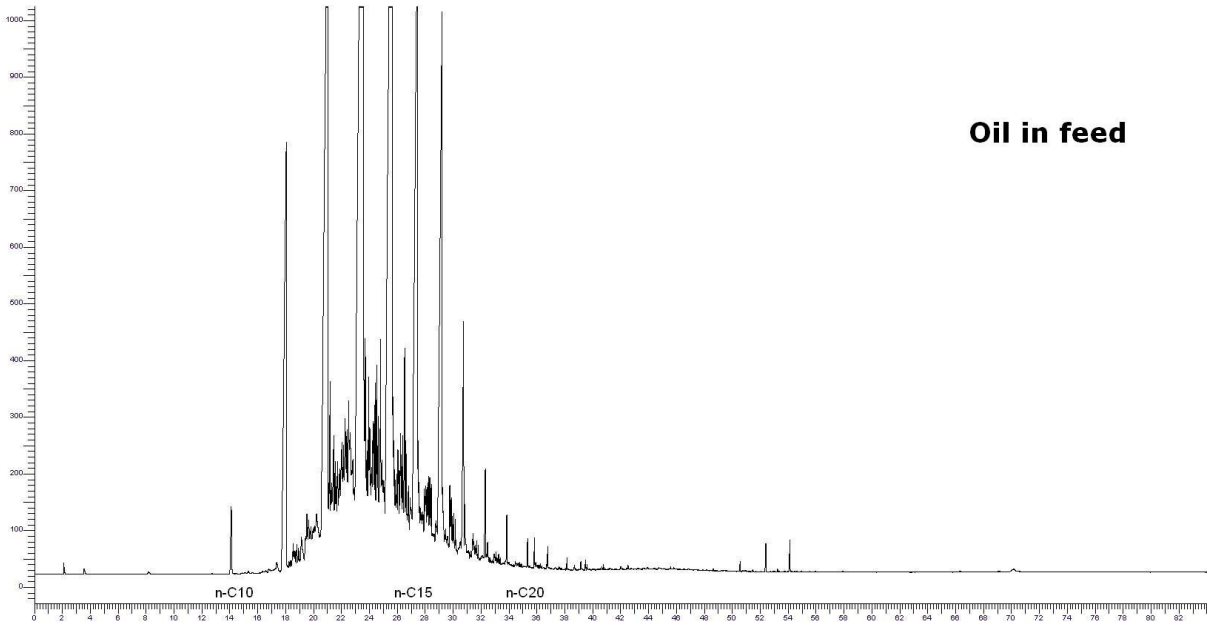

Figure 23 GC-MS profiles of base oil before treatment in the TCC (Valentinetti and Kleppe, 2010)

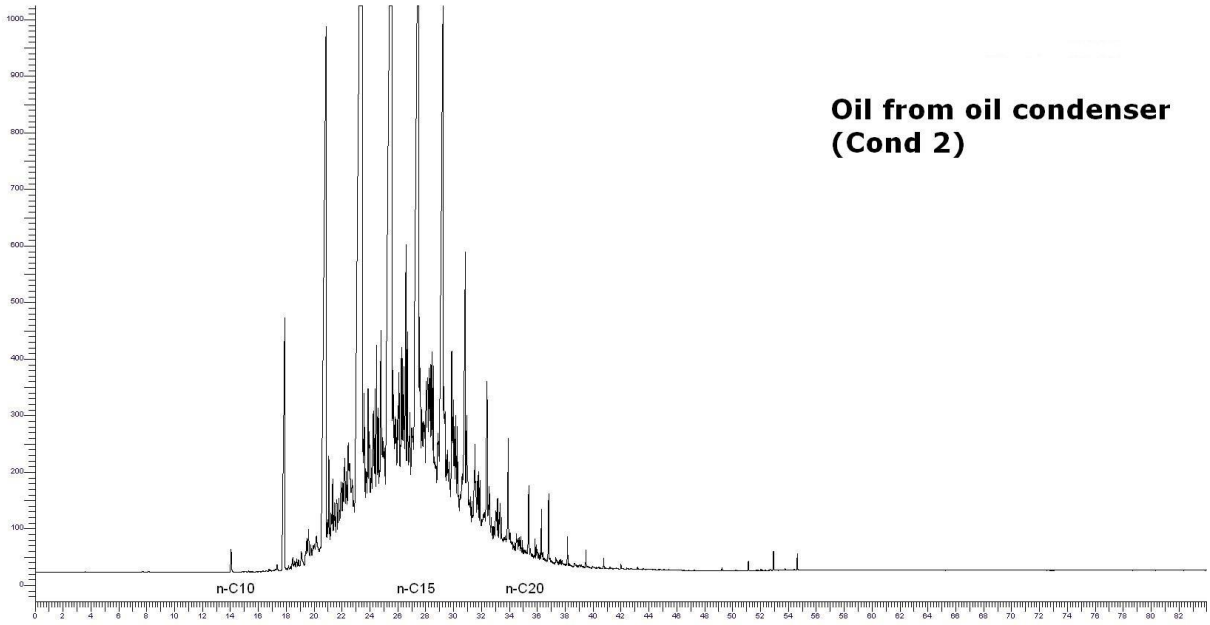

Figure 24 GC-MS profiles of base oil recovered from the TCC (Valentinetti and Kleppe, 2010)

5 References

Argonne (2003) *An introduction to Slurry Injection Technology for the disposal of Drilling Wastes,* Brochure prepared by Argonne National Laboratory for the U.S. Department of Energy, office of Fossil Energy, National Petroleum Technology, Office, September.

Austin, L.G. *The theory of grinding*, Industrial and Engineering Chemistry, vol. 56, no. 11 , 1964. Pp.18-29

Bansal, K.M, and Sugiarto (1991) *Exploration and Production Operations – Waste Management, A comparative overview*: US and Indonesia cases. SPE 54345, SPE Asia Pacific Oil and Gas Conference, Jakarta, Indonesia, April 20-22

BILSTAD, T. 2013. *Thermomechanical Cuttings Cleaner*, Department of Mathematics and Natural Sciences, University of Stavanger, unpublished.

Coalition for Eco-Efficient Comminution, CEEC (2014), *Energy efficient comminution* [ONLINE] Available at: <http://www.ceecthefuture.org/resource-center/?filter=tag-link-33> [Accessed 13 February 2014]

CoorsTek Technical Ceramics (2014) *Ceramic brick wear linings for mining and industrial applications* [Online] Available at: <http://www.coorstek.com/markets/metals_mining/ceramic-linings.php> [Accessed 02 February 2014]

Couslson, J.M., Richardson, J.C., Backhurst, J.R and Harker, J. H. (2002) *Chemical Engineering volume two: Particle technology and separation process,* 5th ed. Pergamon press ISBN 0750644451.

EL-SAYED, A. & KAMAL H, A. TREATMENT OF DRILL CUTTINGS. SPE/EPA/DOE Exploration and Production Environmental Conference, 2001.

Finboroud, A., 2013. *MET 230 Separation technology* [Lecture notes] spring 2013 ed. Department of Mathematics and Natural Sciences, University of Stavanger, unpublished.

Fire Inspection and Prevention Initiative (2014) *Combustible Dust Prevention* [Online] Available at: <http://www.fipibc.ca/about-fipi/ask-an-expert/faq/>

[Accessed 31 January 2014]

Gaudin, A. M., (1971) *Principles of Mineral Dressing* TMH ed., p: 93-120. McGraw-Hill, Inc., New York

GUO, Q., GEEHAN, T. & OVALLE, A. 2007. Increased Assurance of Drill Cuttings Re-Injection-Challenges, Recent Advances and Case Studies. *SPE Drilling & Completion,* 22**,** 99-105.

Hazemag (2014) *Rotors* [Online] Available at: <http://www.hazemag.com/rotors/rotors.htm> [Accessed 07 February 2014]

Homepage Fitzpatrick (2014) *Fitz mill* [Online] Available at: <http://www.fitzmill.com/index.html> [Accessed 28 January 2014]

HAGAN, J., MURRAY, L., MELING, T., GUO, Q., MCLENNAN, J., ABOU-SAYED, A. & KRISTIANSEN, T. Engineering and Operational Issues Associated with Commingled Drill Cuttings and Produced Water Re-injection Schemes. SPE International Conference on Health, Safety and Environment in Oil and Gas Exploration and Production, 2002.

Jeffrey Rader (2014) [Online] Available at: <http://www.jeffreyrader.com/size_reduction/Crushers/AB_Hammermills.cfm> [Accessed 02 February 2014]

Journal of the Southern African Institute of Mining and Metallurgy (2014) *Evaluation of the batch press as a laboratory tool to simulate medium-pressure roller crushers* [Online] Available at: <http://www.scielo.org.za/scielo.php?pid=S0038-223X2012000300009&script=sci_arttext> [Accessed 05 February 2014]

Kennametal Stellite Group (2014) Wear-*resistant, alloy-based materials and components* [ONLINE] Available at: <http://www.stellite.com/> [Accessed 05 February 2014]

KLEPPE, S. "Re-using Recovered Base Oil from OBM Drilling Waste. 2009.

La Crega, M.D., P.L. Buckingham, and J.C. Evans. 1994. *Hazardous Waste Management*. McGraw-Hill, New York, NY

Kuchta, J. M (1985) *Investigation of fire and explosion accidents in the chemical, mining and fuel-related industries*, U.S. Department of the Interior, Bureau of mines; 680, TH9445.C47K8

Microtribodynamics Home (2014), *Friction and Wear Studies of Compressor Surfaces* [ONLINE] Available at: <http://web.mechse.illinois.edu/research/microtribodynamics/sponsors.html> [Accessed 13 February 2014]

MORRIS, J. B. 1981. Drill cuttings treatment apparatus and method. Google Patents.

Natural Resources Canada (2014) *Green Mining Initiative Energy Efficiency* [Online] Available at: <https://www.nrcan.gc.ca/mining-materials/green-mining/8218> [Accessed 07 February 2014]

OSHA Training and Reference Materials (2014) *Flammable and combustible liquids* [ONLINE] Available at: <https://www.osha.gov/dte/library/flammable_liquids/flammable_liquids.html> [Accessed 13 February 2014]

PACE (2014) *Declining ore grades require finer grind size for maximum mineral recovery* [Online] Available at: <http://www.pacetoday.com.au/features/declining-ore-grades-require-finer-grind-size-for> [Accessed 07 February 2014]

Perry, R.H. and Green, D.W., (eds) (1997) *Perry's chemical engineer's handbook* 7th ed., chap. 2, p121 McGraw-Hill ISBN 0-07-049841-5, New York

Perry, R.H. and Green, D.W., (eds) (1997) *Perry's chemical engineer's handbook* 7th ed., chap. 20, p: 11-34 McGraw-Hills ISBN 0-07-049841-5, New York

Petrolyte, 2011. *Drilling mud composition*. [ONLINE] Available at: <http://petrolyte.blogspot.no/2011/03/drilling-mud-composition.html.> [Accessed 04 March 2014].

PISZCZ, K., PTASZYŃSKA, A. & HUPKA, J. Method of managing drill cuttings from shale gas formations,2009.

PROCES (2014) *Ball mills* [Online] Available at: <http://www.jmeech.mining.ubc.ca/MINE290/proces/ball_mill.php> [Accessed 28 January 2014]

QUINTERO, L. & LIMIA, J. 2003. Treatments for drill cuttings. Google Patents.

R. L. Earle (2014) *Unit operations in food processing* [Online] Available at: <http://www.nzifst.org.nz/unitoperations/sizereduction1.htm>

[Accessed 05 February 2014]
RQI Inc. (2014) *Rotor School* [Online] Available at: <http://www.rotors.com/rotor-school/6.html>[Accessed 07 February 2014]
RUSSULA Inc. (2014) *Drive selection for rolling* [Online] Available at: <http://www.russula.com/articles/article-04.php> [Accessed 10 February 2014]
Sagmilling Homepage (2014) *Mill critical speed determination* [Online] Available at: <https://sagmilling.com/tools_millspeed> [Accessed 07 February 2014]
SAMPLE JR, T. E. 1979. Method for thermally treating oil well drill cuttings. Google Patents.
Scomi Oil tools (2014) *Drill Cuttings Bioremediation* [ONLINE] Available at: <http://www.scomigroup.com.my/core/DWM/pdf/treatmentDisposal/Bioremediation_1208.pdf.>[Accessed 03 March 2014].
Shadizadeh, S. R., Zoveidavianpoor M., Samsuri A. (2012) *Overview of Environmental Management by Drill Cutting Re-Injection Through Hydraulic Fracturing in Upstream Oil and Gas Industry*,[Online] Available at:< http://dx.doi.org/10.5772/45828> 1093-1103. ISSN: 978-953-51-0682-1 [Accessed 05 March 2014].
Sinnot, R.K. (2003). *Chemical Engineering Design*, 3rd ed., Vol., 6, p: 807-870 Elsevier Butterworth Heinemann, Oxford
THERMTECH AS. General Technical Files and Handbook. Jacob Kjødes vei 15, 5232 Paradis, Norway, 2013.
VALENTINETTI, R. AND KLEPPE, S. "Re-using Recovered Base Oil from OBM Drilling Waste. 2010.
Walas, S.M. (1990). *Chemical Process Equipment: Selection and Design*. P: 339-350 Butterworth- Heinemann, Washington street Newton.
Wills, B. A., (2006). Mineral Processing Technology: *An introduction to the practical aspects of ore treatment and mineral recovery*, 7th ed., Chap. 7, Elsevier Science & Technology Books ISBN: 0750644508.
Wisegeek (2014) *Spalling* [Online] Available at: <http://www.wisegeek.com/what-is-spalling.htm> [Accessed 02 February 2014]

PART TWO: MODELLING AND SIMULATION

1 CASE STUDY ONE: Response time of temperature change inside the process mill

1.1 Introduction

Heat is generated in the process mill by friction. The quantity of heat generating in the process mill is usually controlled by measuring the temperature. Control of the temperature level (or value) is necessary to keep the process optimal. The temperature is recorded by a thermocouple mounted to the stator. A temperature transmitter sends signals that are readable on the programmable logic control (PLC) interface. There is usually a delay to recognise a change in temperature at a specific time in the process mill. Thus if there is any change in the temperature, the actual temperature in the process mill will be different from what is being shown on the PLC interface. This chapter is to investigate the effect of relevant parameters on this delay by using finite element method.

1.2 FINITE ELEMENT (FE) MODELLING

In order to make a FE model the followings need to be defined:

1.2.1 Material and Process Parameters

The process mill is constructed from structural steel in this study and the liner is tungsten carbide. The physical properties of the used material are given in Table 3 and

Table 4. The process parameters in this case are the operating process temperature, temperature increase (a boundary condition) and thickness of stator (which is constant, 20 mm).

Table 3 Physical properties of the structural steel (Source: COMSOL Multiphysics, 2013)

Name	Value	Unit
Specific heat capacity	475	J/(kg.K)
Thermal conductivity	44.5	W/(m.K)
Density	7850	Kg/m^3

Table 4 Physical properties of tungsten carbide (Source: COMSOL Multiphysics, 2013)

Name	Value	Unit
Thermal conductivity	60	W/(m*K)
Density	15000	Kg/mˆ3
Specific heat capacity	200	J/(kg*K)

1.2.2 Finite Element Parameters

The finite element simulation was performed in 2D using COMSOL multiphysics software. The physics used in this simulation is the "Heat Transfer in Solids". The free triangular mesh generator was used with 492 triangular elements, 68 edge elements and 4 vertex elements. This corresponds to the predefined mesh size of "finer". Figure 25 below is the meshed geometry build for this study. The software solves the following equation to calculate the transient heat transfer by conduction in the sample material:

$$\rho C_p \frac{\partial T}{\partial t} + \rho C_p u \cdot \nabla T = \nabla \cdot (k \nabla T) + Q$$

Where ρ is the density, C_p is the heat capacity at constant pressure, Q is the heat source other than viscous heating, u is the velocity vector, T is the temperature, t is time and k is the thermal conductivity (COMSOL Multiphysics, 2013).

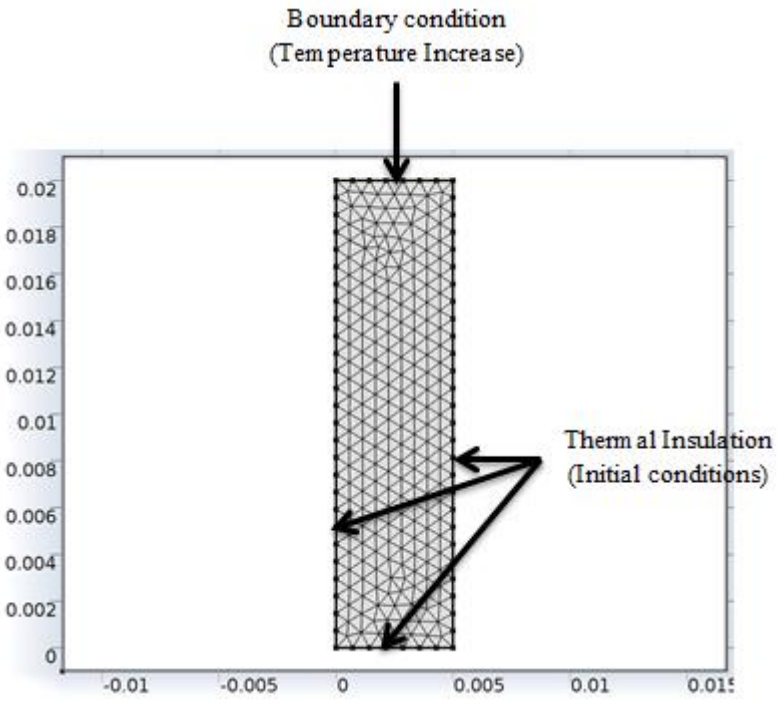

Figure 25 Meshed geometry of the studied sample

1.2.3 Boundary and Initial Conditions

Three out of the four edges of the sample were defined as thermally insulated. The temperature increase was applied to the fourth edge. The initial temperature was applied on the geometry (as shown in Figure 25).

1.3 Case Design

Three different process temperatures (200°C, 350°C and 500°C) of the process mill were considered. The entire geometry was set to each process temperature and then a boundary condition (the process temperature + the temperature increase) was applied at the boundary representing the internal surface of the process mill.

Two - three point probes were defined on the geometry (as shown in Table 6) within the thickness of the steel. A point probe represents a thermocouple tip position. The time taken for the point probes to reach the same temperature as that of the heated boundary was measured. The Table 5 describes the process parameters at different operating scenario in the process mill as defined in this simulation.

Table 5 Studied parameters values at the different scenarios

Parameter	Value
Process temperature (°C)	200,350,500
Temperature Increase (°C)	50, 75, 100
Material Thickness (mm)	20
Material	Steel with/without liner
Probe point distance from the surface (mm)	2,5,10

1.4 The Simulation Methodology

The study was done in two steps:

1. *Parameters effect without liner*: the aim of this step is to study the effect of the process parameters and the thermometer tip position on the lag in temperature transmission. The studied parameters are:
   i. Process temperature
   ii. Temperature increase
   iii. Thermocouple position as described in Table 6

2. *Parameters effect with Tungsten carbide liner inside the process mill*: internal surface of the process mill is usually hard-faced. The physical properties of the liner are shown in
3. Table 4. The liner thickness was considered as a studied parameter in this step. Otherwise, the conditions were the same as the previous step.

Table 6 Thermocouple tip position within the stator

Probe point	Distance with reference to the liner surface (mm)	Distance with reference to the steel surface (mm)
1	2	2
2	5	5
3	10	10

Table 7 Studied parameters for the process mill without liner

Simulation Case No.	Initial Conditions [Process temperature (^{o}C)]	Boundary Condition [temperature Increase (^{o}C)]
1	200	50
2		75
3		100
4	350	50
5		75
6		100
7	550	50
8		75
9		100

1.5 Results

As mentioned, at first stage, the results are based on a model without considering liner. A typical result of such a simulation is shown in Figure 26.

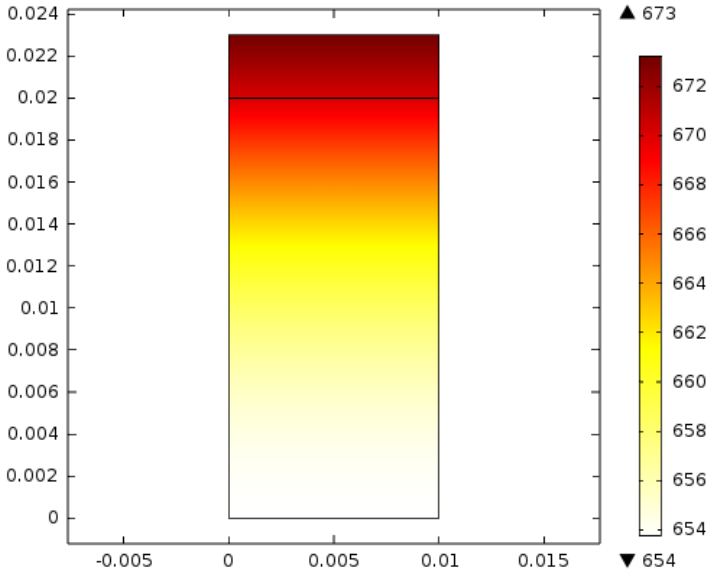

Figure 26 Temperature profile of the studied geometry after 20 s

The early simulation results showed that the nominal process temperature has no effect on the response delay. The significant effect belongs to the temperature increase (change) in the process. The results regarding to this parameter are shown in Figure 27; the delay duration increases by increasing the parameter. The response delay raises about 9.5 sec by changing the temperature increase from 50 °C to 100 °C, regardless of the probe position (5 mm or 10 mm in this study). Putting the probe at 5 mm from the hot surface decreases the response delay 8 sec.

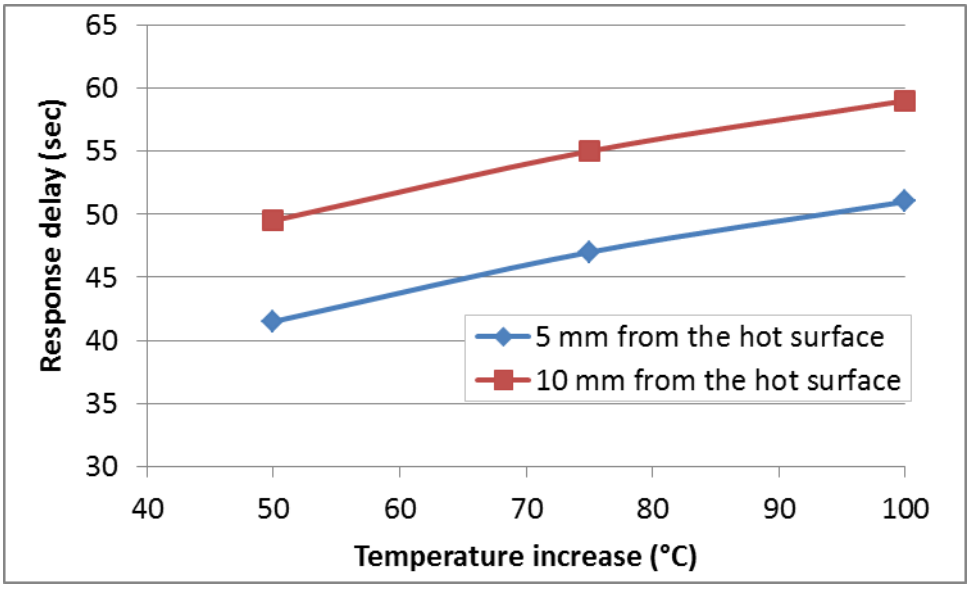

Figure 27 The effect of the temperature increase on temperature transmission delay for the process mill without liner

While using a 3 mm tungsten carbide liner, makes the effect of the temperature increase and the probe position stronger (as shown in Figure 28) the probe position effect is 4 sec (50%) more than the case without liner and 2.5 sec longer response delay for the temperature increase from 50 °C to 100°C.

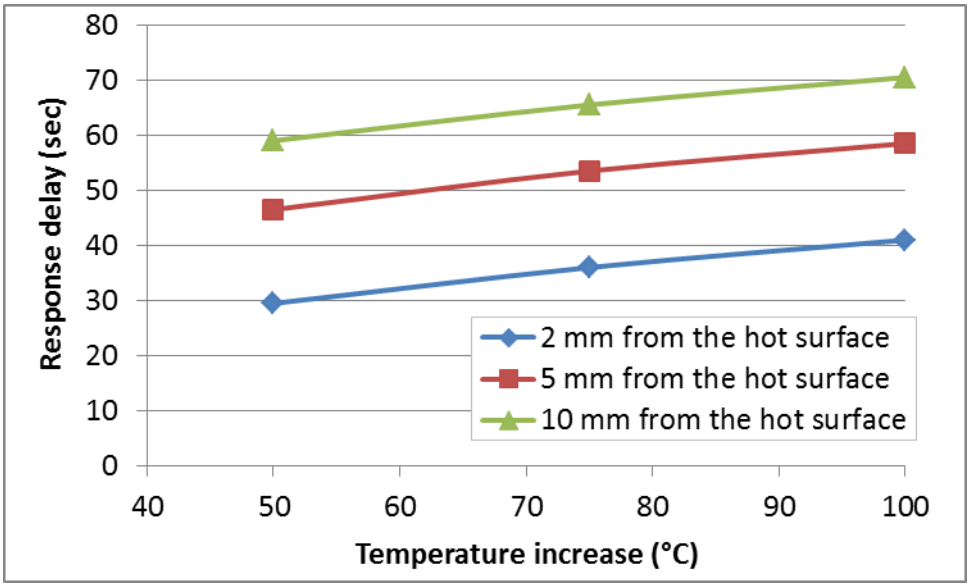

Figure 28 The effect of the temperature increase on temperature transmission delay for the process mill with 3 mm liner

Increasing of the liner thickness increases the response delay. In the studied cases, the thickness effect is significantly depending on the probe position. When the probe is located at 2 mm from the hot surface and the thickness is changed from 3 mm to 6 mm, it increases the response delay 4 sec, while a probe at 10 mm from the hot surface gives 9 sec extra delay duration.

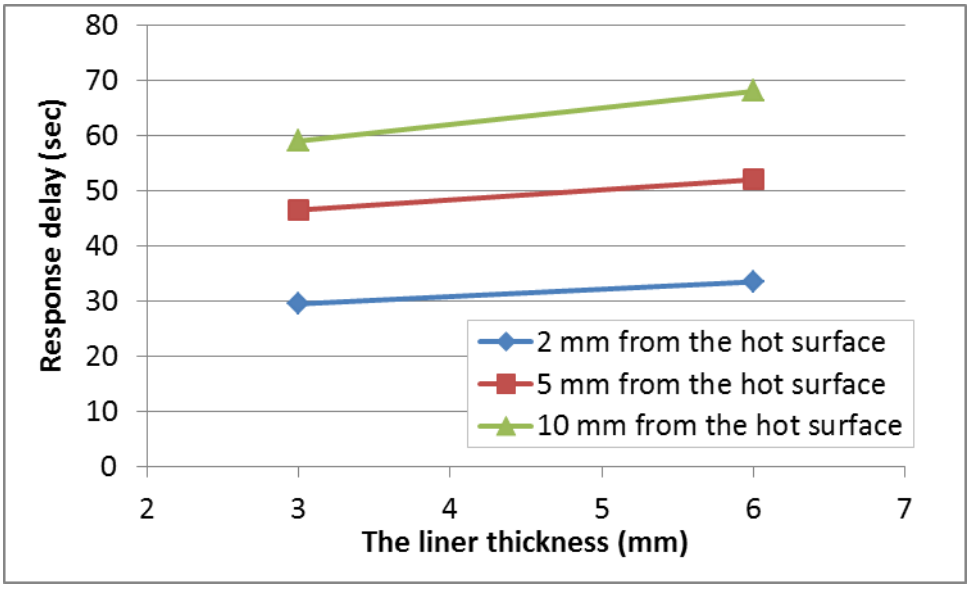

Figure 29 The effect of the liner thickness on the response delay

1.6 Discussion

The results show that the transmission time delay is independent on the initial process temperature but rather on the increase in the temperature. It can be deduced from the results that increasing the process temperature by 50 °C takes approximately 42 sec for the thermocouple tip mounted at 5 mm from the hot surface to detect the rise in process temperature. While the thermocouple tip situated at 10 mm from the surface takes 50 sec to sense the 50 °C increase in process temperature.

Under normal operating conditions, the process mill discharges the processed solids every three minutes. Comparing the effect of the Initial and boundary conditions on temperature transmission delay, assuming that the process mill is without liner, it shows clearly that the transmission delay is significant.

The temperature increase is obviously detected quicker if the thermocouple tip is located at the closer position to the hot surface but the response delay by changing the temperature increase is almost the same (as two curves in Figure 27 are parallel).

Adding a liner inside the process mill practically is normal as it extends the life of the process mill by protecting the surface against wear. But this can increase the response delay further more. As using 3 mm tungsten carbide liner increases the response time up to 50%. The liner thickness is also important regarding to the response time as it increases the response time because of its higher conductivity comparing with steel. In practice, increasing the liner thickness makes limitation on the thermocouple position from the internal surface; as it is not easy (and recommended) to put the thermocouple in the liner.

1.7 Conclusion

A response time to the temperature changes inside the process mill was developed and it was shown that all studied parameters except the process temperature have effect on the response delay. It was illustrated that changing the parameters can effect on the response delay but can't eliminate it. So two conclusions are provided accordingly:

1. Being aware of any temperature change in advance; meaning any small changes in the process temperature to be considered important and the control system shall react to such change. Specifically if the temperature change continues.
2. Finding a way to mount the thermocouple tip inside the process mill.

1.8 References

COMSOL, Inc. (2013) *COMSOL Multiphysics*®, Version 4.4

2 CASE STUDY TWO: The effect of relevant parameters on the velocity magnitude and efficiency of the process mill

2.1 Introduction

The TCC converts kinetic energy from the rotating arms of the hammer mill into thermal energy. The rotating hammers generate a velocity pattern for the cutting in the process mill. The velocity pattern is such that there are regions of minimum velocity magnitude and maximum velocity magnitude.

This study is to investigate the velocity pattern and the velocity magnitude of the cuttings that is being processed in the process mill as a result of the rotating hammers. The velocity pattern and magnitude will be studied by varying some of the process parameters, operating parameter and design parameters as shown in Table 9.

The effect of some properties of the drill cuttings such as the dynamic viscosity on the velocity magnitude will also be covered. Finally, the effect of the velocity magnitude and the velocity pattern on the efficiency of the process mill will be studied.

2.2 Theory of the Rotating Machinery

Rotating Machineries are equipment with rotating parts and can be operated in laminar flow or turbulent flow conditions. Examples of rotating machinery are stirred tanks, mixers, and pumps (Greenspan, 1990). The Navier-Stokes equations formulated in a rotating coordinate system are:

$$\frac{\partial \rho}{\partial t} + \nabla \cdot (\rho v) = 0$$

$$\rho \frac{\partial v}{\partial t} + \rho(v \cdot \nabla)v + 2\rho\Omega \times v = \nabla \cdot [-pI + \tau] + F - \rho\left(\frac{\partial \Omega}{\partial t} \times r + \Omega \times (\Omega \times r)\right)$$

Where v is the velocity vector in the rotating coordinate system, r is the position vector and Ω is the angular velocity vector, ρ is the density (kg/m3), τ is the viscous stress (Pa), F is the volume force vector (N/m3). The relation between the velocity vectors in the non-rotating coordinate system, u and the velocity vector in the stationary coordinate system, v is given by (Batchelor, 2000):

$$u = v + \frac{\partial r}{\partial t}$$

The Rotating Machinery, fluid flow interfaces solves the Navier-Stokes equations, but it is reformulated in terms of a non-rotating coordinate system. Thus they solve for u. This is achieved by invoking the Arbitrary Lagrangian-Eulerian Formulation (ALE) machinery (Brucato *et al.*, 1998). The Navier-Stokes equations on rotating domains then become:

$$\frac{\partial \rho}{\partial T} - \frac{\partial x}{\partial T} \cdot \nabla\rho + \nabla \cdot (\rho u) = 0$$

$$\rho\left(\frac{\partial u}{\partial T} - \frac{\partial x}{\partial T} \cdot \nabla u\right) + \rho(u \cdot \nabla)u = \nabla \cdot [-pI + \tau] + F$$

The derivative operator ∂ρ/∂T is the mesh time derivative of the density whiles ∂u/∂T is the mesh time derivative of the velocity. The variable TIME replaces t as the variable for time.

The angular frequency, ω is prescribed by the input for the rotating domain. The physics interfaces set up an Ordinary Differential Equation (ODE) variable for the angular displacement ω in order to calculate for Ω. The equation for ω is

$$\frac{d\omega}{dt} = w$$

Ω, is defined as ω times the normalized axis of rotation. The axis of rotation in 2D is the z direction, while it is specified in the rotating domain features for 3D geometry. The ordinary Navier-Stokes equations are solved in non-rotating domains. The rotating and fixed parts need to be coupled together by an identity pair, where a continuity boundary condition is applied (Greenspan, 1990).

2.2.1 Frozen Rotor

The Navier-Stokes equations on rotating domains can be solved using a time dependent study which can be computationally expensive. The frozen rotor approach however assumes that the flow in the rotating domain, expressed in the rotating coordinate system, is fully developed. The frozen rotor study reduces the Navier-Stokes equations to:

$$\nabla \cdot (\rho v) = 0$$

$$\rho(v \cdot \nabla)v + 2\rho\Omega \times v = \nabla \cdot [-pI + \tau] + F - \rho\Omega \times (\Omega \times r)$$

Frozen rotor is both a study type and an equation form. A frozen rotor study step solves a rotating machinery model assuming a "rotating" domain, but the "rotating" domains do not rotate at all. Boundary conditions remain transformed as if the domains were rotating, but the domains remain fixed, or frozen, in position (Batchelor, 2000).

The rotating machinery, fluid flow interfaces solve for the velocity vector in the stationary coordinate system, u, rather than for v in the time-dependent case. The frozen rotor study step defines a parameter TIME, which by default is set to zero. This is represented by the equation (Brucato *et al.*, 1998).

$$\omega = wTIME$$

Since TIME is a parameter and x is a function of TIME, ∂x/∂T evaluates to its correct value. Finally, ∂ρ/∂T = 0 and the mesh time derivative of the velocity is replaced by:

$$\frac{\partial u}{\partial T} = \Omega \times u$$

In non-rotating domains, the ordinary stationary Navier-Stokes equations are solved. The frozen rotor study step uses a stationary solver to solve the resulting equation system. In most cases however, there is no steady state solution to the rotating machinery problem but rather a pseudo-steady state where the solution varies periodically around some average solution (Batchelor, 2000).

In these cases, the frozen rotor approach gives an approximate solution to the pseudo-steady state. The approximation depends on the position in which the rotor is frozen. An estimate of the effect of the rotor position can be obtained by making a parametric sweep over TIME (Batchelor, 2000).

Starting from a frozen rotor solution, the pseudo-steady state can be reached within a few revolutions, while staring from u=0 can require tens of revolutions (Torré *et al.*, 2007).

2.3 FINITE ELEMENT MODELLING

The finite element modelling was done by defining the materials and process parameters, finite element parameter, boundary and initial conditions as required by the software in other to facilitate the simulation.

2.3.1 Materials and Process Parameters

The material whose velocity magnitude will be studied is the drill cuttings that are treated by the process mill. The drill cuttings compose of 15% water, 15% oil and 70% solids (Kleppe, 2009). The properties of the drill cuttings are given in the Table 8. Table 9 describes the parameters of interest, their references in the study and the range in each scenario during the simulation.

Table 8 The Physical properties of drill cuttings (Source: Santoyo *et al.*, 2001)

Property	**Value**	**Unit**
Density	1040	Kg/m^3
Dynamic Viscosity	14×10^{-3}	Pa.s

2.3.2 Finite Element Parameters

The finite element simulation was performed in 3D using COMSOL multiphysics software. The physics used in this simulation is the "Rotating machinery, Laminar flow (rmspf)". The free tetrahedral mesh generator was used with 198720 tetrahedral elements, 3182 edge elements, 34302 boundary elements and 176 vertex elements. This corresponds to the predefined mesh size fine with minimum element quality of 0.1214. Figure 30 represents the mesh element build for the geometry. The software solves the following Navier-Stokes equations to calculate for the velocity magnitude for the drill cuttings in the process mill during the simulation (COMSOL multiphysics, 2014):

$$\frac{\partial \rho}{\partial t} + \nabla \cdot (\rho v) = 0$$

$$\rho \frac{\partial v}{\partial t} + \rho(v \cdot \nabla)v + 2\rho\Omega \times v = \nabla \cdot [-pI + \tau] + F - \rho\left(\frac{\partial \Omega}{\partial t} \times r + \Omega \times (\Omega \times r)\right)$$

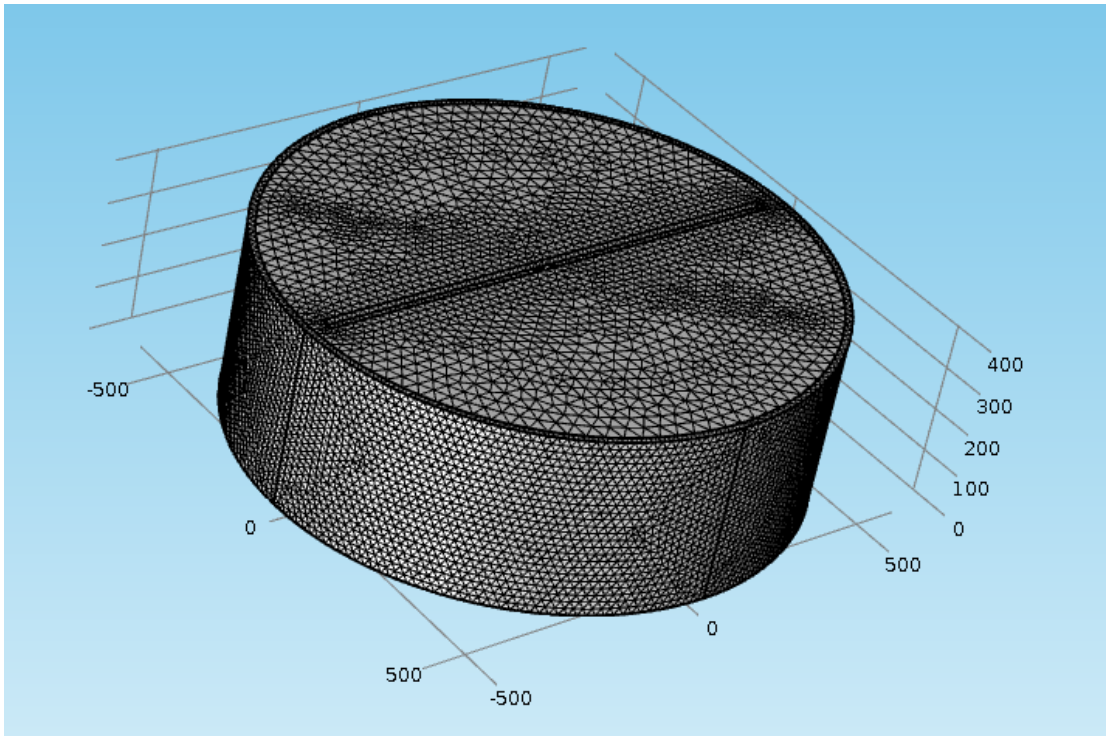

Figure 30 Meshed geometry of the studied process mill model

2.3.3 Boundary and Initial Conditions

The boundary conditions were defined such that, there is a clear distinction of the rotating wall and the fixed wall as shown in Figure 31. The rotating wall describes the rotor and the hammers inside the stator. The fixed wall boundary was however defined to represent the stator.

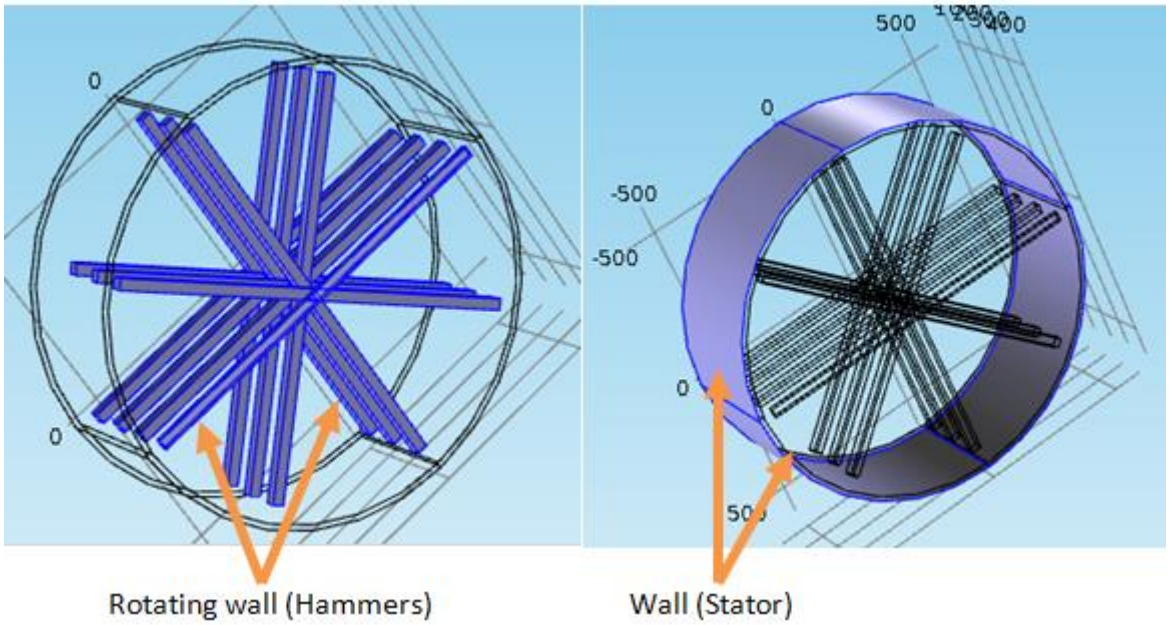

Figure 31 The rotating wall and the fixed wall of the Process mill model

2.4 Case Design

The Process Mill was modeled into rotationally invariant geometries. The finite element module of the process mill that was created comprised of a stator and a rotating hammers. The hammers rotate from position 1 to 2 as shown in Figure 32.

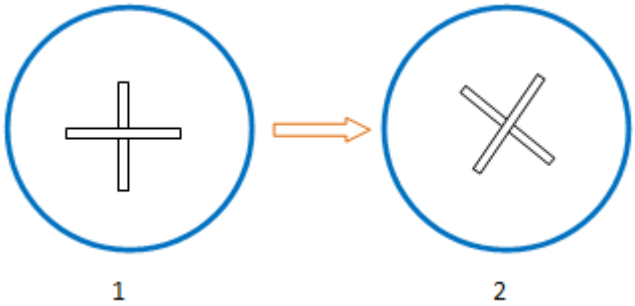

Figure 32 The modelling procedure in a Rotating Machinery for fluid flow

The geometry of the process mill was modeled into two domains i.e. fixed and rotating parts. An assembly was formed for the geometry in order to create identity pairs, which makes it possible to treat the domains as separate parts in the assembly. Rotating Domain features were applied to the model. The fluid properties were specified as drill cuttings and boundary conditions were applied. Flow Continuity was applied to the assembly pairs and a pressure point constraint added. After applying the appropriate boundary conditions, the mesh was created followed by computation of the simulation.

2.5 The Simulation Methodology

The study was performed in two steps:

1. *Reference Simulation*: the aim of this step is to set a control for the subsequent simulations. The reference simulation was done to model the process mill such that the studied parameters will have values equivalent to that of the process mill. The similarities in the parametric values will help to formulate a control for the subsequent models and to compare the effect of the studied parameters on the efficiency of the process mill. The parameters that were studied are:
    i. Number of hammers
    ii. Rotational frequency
    iii. Dynamic viscosity
    iv. Thickness of Hammers
    v. Angle of inclination between adjacent hammers and
    vi. Distance between adjacent hammers as described in the Table 9.
2. *Studying the selected parameters and their effect on the velocity magnitude and the efficiency of the process mill*: the selected parameters were altered per definition in Table 9. The values of the selected parameters were varied in other to study the effect of these parameters on the velocity distribution and velocity magnitude of the drill cuttings in the process mill. Otherwise the conditions were the same as the reference simulation. Finite element modules were simulated with boundary conditions comparable with that of the process mill.

Table 9 The studied parameters of the process mill

Parameter	Reference	Cases
Number of Hammers	13	3 & 5
Rotational frequency, (revolution per seconds)	10	2 &100
Dynamic viscosity (Pa.s)	14×10^{-3}	5×10^{-3} & 30×10^{-3}
Thickness of hammer (mm)	30	10 & 70
Angle between adjacent hammers (Degree)	45	90
Distance between Adjacent hammers (mm)	0	30 & 50

2.6 Results and Discussion for Reference Simulation

The set of figures and curves below displays the results of the simulation and computation of the reference model. Figure 33 shows a typical plot of the simulation results and the comparison between the velocity distributions in the process mill when it is operated under the reference conditions (See Table 9). The relative change in velocity distribution and velocity magnitude is observed as the velocity magnitude increases from the centre of the rotor to the tip of the hammers.

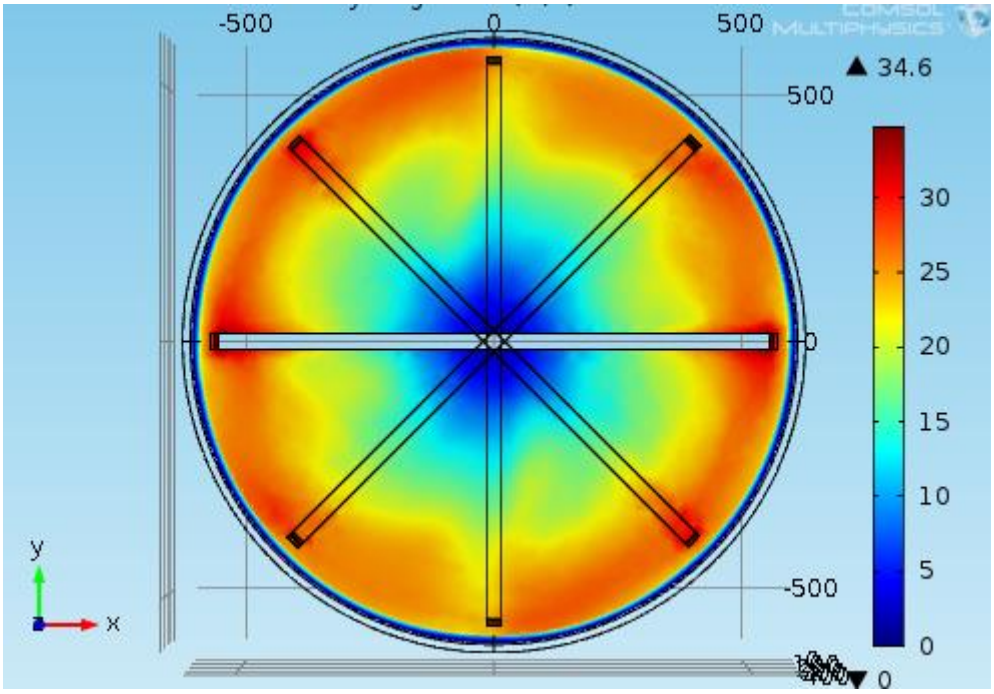

Figure 33 Velocity magnitude of the reference simulation

The velocity distribution within the process mill affects the distribution of the drill cuttings in the process mill during operation. This shows that the change in velocity magnitude has a significant effect on the performance of the Process Mill.

The velocity magnitude changes along any diameter of the process mill. The maximum velocity magnitude was observed around the tip of the hammers (orange – red colour on the Figure 33), whereas the minimum velocity magnitude was observed along the stator internal wall and around the rotor (blue colour on the Figure 33).

Figure 34 shows the cut lines defined at the midpoint of the process mill model. The cut lines were defined to aid the study of the velocity magnitude distribution along desired directions in the process mill. Hence, the cut lines were defined through the vertical, horizontal and diagonals of the process mill model, as shown in Figure 34.

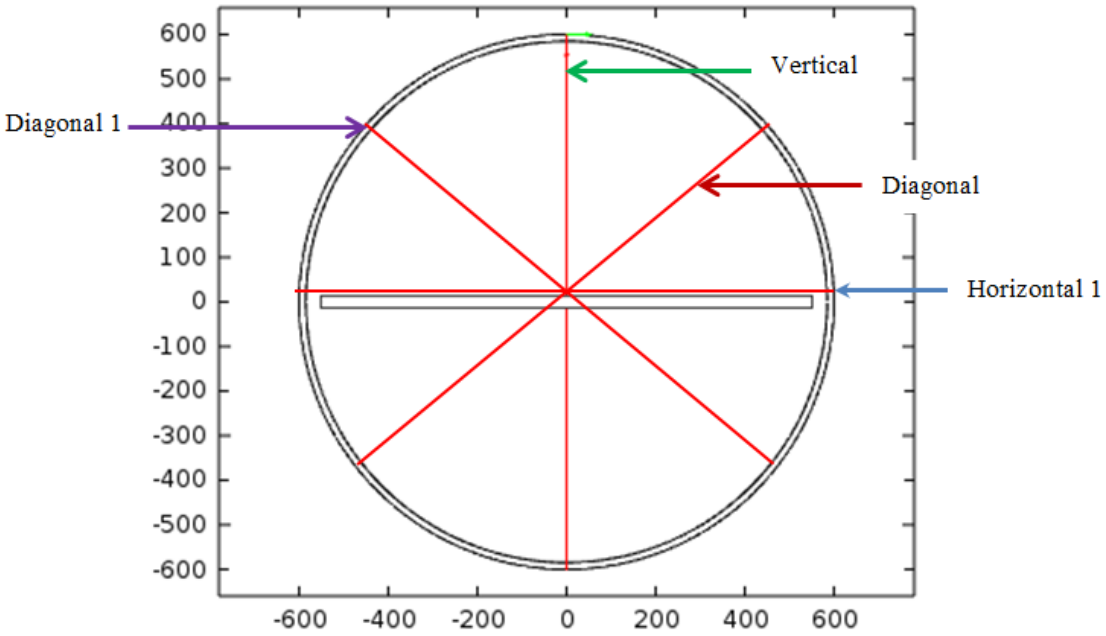

Figure 34 Defined cut lines within the process mill

Figure 35 shows the velocity magnitude of the drill cuttings in the process mill model and the critical speed above which the drill cuttings is fluidized. It can be observed from that above a critical velocity of 2.5 m/s the drill cuttings in the process mill model will be fluidized.

It can be deduced from Figure 35 that the maximum velocity magnitude that was observed on the **horizontal 1**cutline is 33.7 m/s. The plot shows that the material in the process mill model has the maximum velocity magnitude at the clearance between the horizontal hammer tip and the stator. This is because the maximum critical velocity occurs at the hammer tip. The minimum velocity magnitude recorded on the **horizontal 1** cutline is 1.2 m/s.

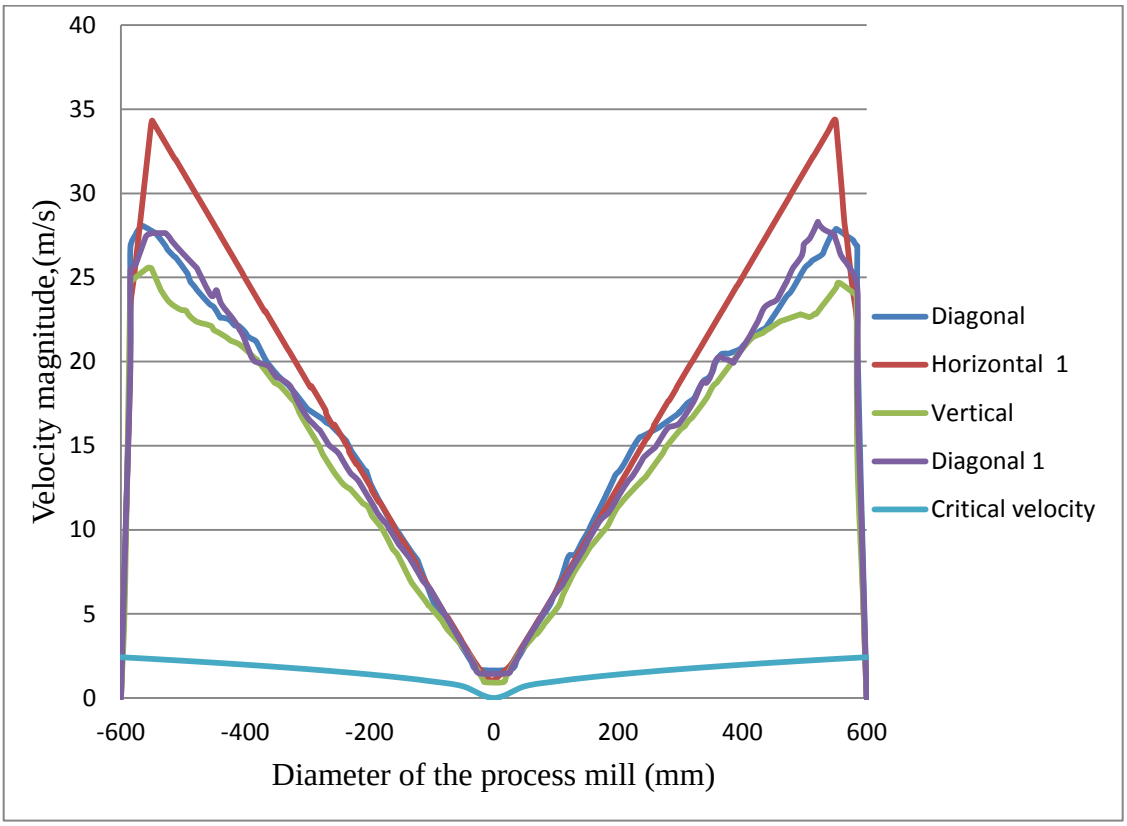

Figure 35 The critical velocity on the defined cut lines

Considering the cutline defined through the diagonal of the process mill model, it recorded a maximum velocity magnitude of 27.8 m/s, what was recorded in between the stator and the hammer tip at the diagonal section of the process mill. The minimum velocity magnitude recorded for this cutline is 1.7 m/s and it occurs around the rotor which is at the middle of the process mill drum.

The plot of the velocity distribution along the vertical cut line shows a maximum velocity magnitude of 25.6 m/s and a minimum velocity magnitude of 1.1 m/s (see Figure 35). The maximum velocity magnitude was also recorded in between the stator and the hammer tip, whereas the minimum velocity magnitude was recorded around the middle of the process mill drum around the rotor.

The drill cuttings cannot move about the axis of the rotor when the rotor is rotating below the critical speed. This will cause the drill cuttings to fluidize as the critical speed occurs at the rotational velocity at which the centrifugal forces equal the gravitational forces at the mill's stator inside surface.

At the critical speed the drill cuttings will not fall away from the stator inside surface. Thus, the cuttings will be fluidize and suspended between the hammer tip and the stator inside surface.
Comparing the velocity magnitude of the drill cuttings in the process mill model at the define cut lines, it can be deduced that the velocity pattern of the material is distributed in such way that the maximum velocity magnitude occurs at the hammer tip, while the minimum velocity magnitude occurs at the middle of the process mill drum around the rotor (see Figure 35).

It can be observed from Figure 33 that the velocity pattern varies with the position of the hammer as it rotates in the clockwise direction with the horizontal positions recording the maximum velocity magnitude of 34.6 m/s compared to the vertical positions, which recorded the least maximum velocity magnitude of 25.6 m/s. This depicts that the velocity pattern is relevant for the optimal operation of the process mill. The velocity magnitude is relevant because fluidisation of the drill cuttings being treated in the process mill can be achieved at velocities above the critical speed.

2.7 Parametric Study

The simulation was done for the selected parameter and the effect on the velocity magnitude was analysed.

2.7.1 Effect of Number of Hammers

To study the effect of the number of hammers on the velocity magnitude and velocity distribution, two simulations were performed, each with explicitly specified number of hammers. Figure 36 **(a)** shows results of the model with 3 hammers, while Figure 36 **(b)** depicts the results of the 5 hammers model on the velocity distribution.

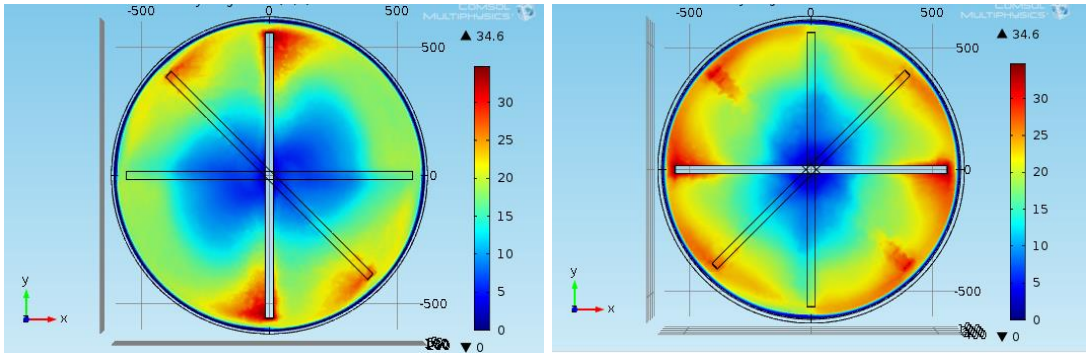

(a) Three hammers **(b)** Five hammers

Figure 36 The effect of the number of hammers on the velocity distribution in the process mill at the middle hammer

The velocity distribution in Figure 36 shows that the model with 5 hammers gives a uniform velocity distribution compared with that of the 3 hammers. However, the velocity distribution of the reference model is the most uniform compared to that of the model with 3 hammers and the model with 5 hammers.

The differences in the velocity distribution will also affect the efficiency of each model compared to the reference model. The non-uniformity in the velocity distribution will decrease the efficiency of the process mill. This will affect the heat generation and hence decrease the efficiency of a design with less number of hammers compared to the reference model.

The rate of size reduction as well as heat generation will be minimal in the model with 3 and 5 hammers compared to the reference model, which has 13 hammers. So, the model with more hammers will have the greatest impact with the drill cuttings, thereby increasing the friction between the hammer tips and the drill cuttings and hence an effective increase in the heat generation.

Figure 37 shows the effect of the number of hammers on the velocity magnitude of the drill cuttings inside the process mill.

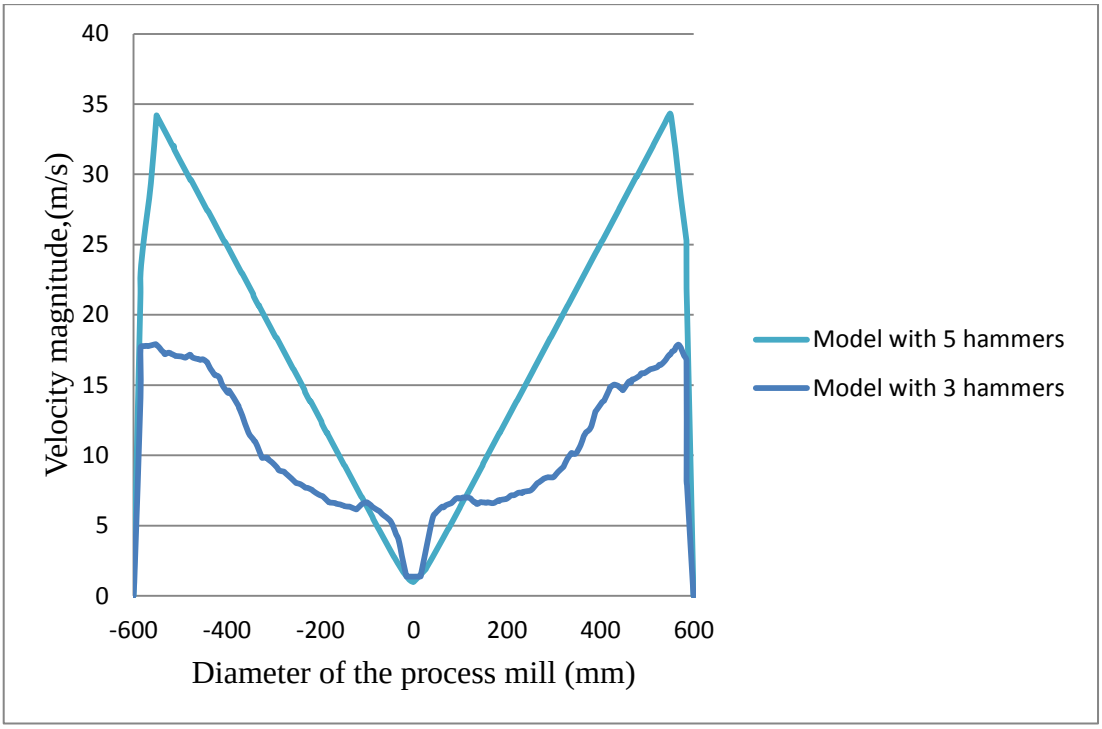

Figure 37 The velocity magnitude for the model with only 3 hammers and the model with 5 hammers at the middle hammer

It can be observed from Figure 37 that the model with 5 hammers has a higher velocity magnitude (33.5 m/s) compared to the model with 3 hammers (17.7 m/s). However, the reference model recorded the highest velocity magnitude amongst the three models.

2.7.2 Effect of Rotational Frequency

Figure 38 **(a)** shows the maximum velocity magnitude of 6.6 m/s while Figure 38 **(b)** gives a maximum velocity magnitude of 336 m/s. This is the recorded maximum velocities as a result of operating the process mill model at rotational frequencies of 2 revolutions per second and 100 revolutions per second respectively.

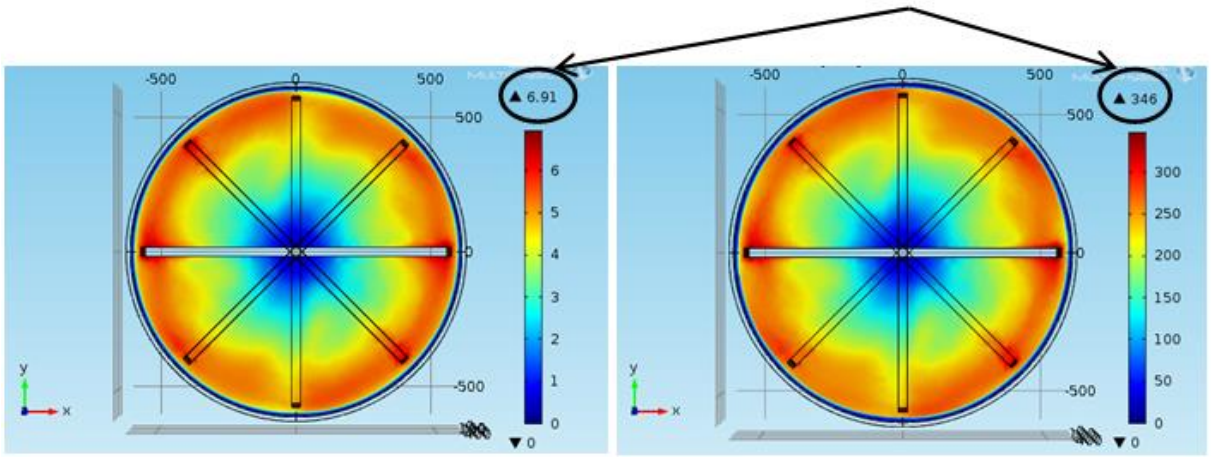

Figure 38 The effect of the rotational frequency on the velocity distribution in the process mill
(a) 2 revolutions per second **(b)** 100 revolutions per second

The uniform velocity distribution observed in Figure 38 **(a)** and **(b)** is due to the equal number of number of hammers in each model. Figure 39 is the plot comparing the effect of rotational

frequency on the velocity magnitude of the drill cuttings in the process mill. Comparing the effects of the rotational frequency on the velocity magnitude, it can be deduce from Figure 39 that the effect of 100 revolutions per second on the velocity magnitude is 10 times the effect of 10 revolutions per second on the velocity magnitude, which confirms to theory: $= \pi \times D \times n$, where V is the velocity (m/s), n is the rotational frequency (revolutions/second).

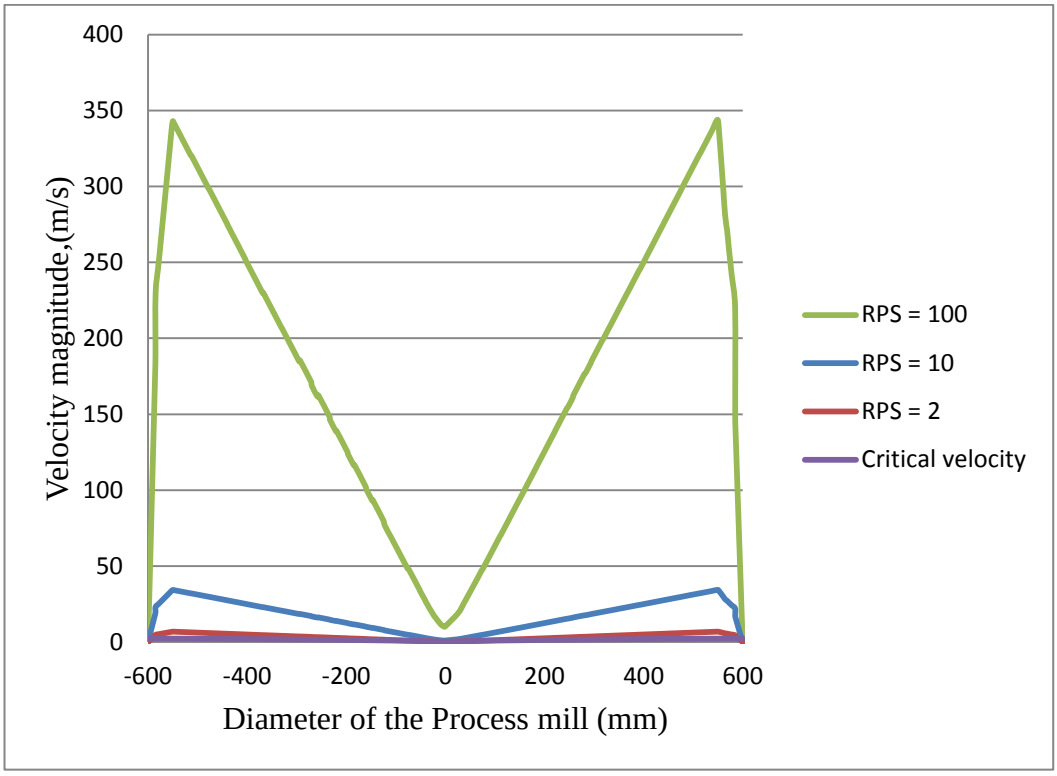

Figure 39 The velocity magnitude for models with rotational frequency of 2, 10, and 100 (in revolution per seconds, RPS)

Operating the process mill at high rotational speed may result in vibrations that can cause the machine to break. At a rotational speed of 100 rps, careful considerations must be given to the design of process mill, the material used in construction and the fabrication of all components.

2.7.3 Effect of Dynamic Viscosity

Operating conditions and hammer design can affect the slurry distribution within the process mill. To help understand the effect of the viscosity of the feed material in the process mill two simulations were done with specific dynamic viscosity for the feed material. Figure 40 **(a)** and **(b)** show the effect of the dynamic viscosity on the velocity magnitude and velocity distribution in the process mill models.

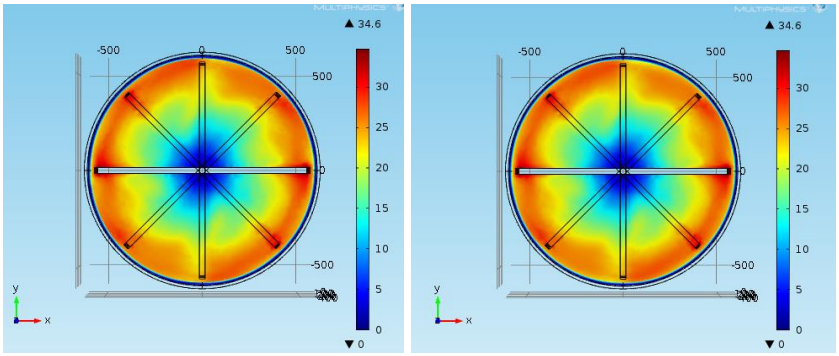

(a) Viscosity = 5×10^{-3} Pa.s **(b)** Viscocity =30×10^{-3} Pa.s

Figure 40 The effect of the dynamic viscosity on the velocity distribution in the process mill

The effect of the dynamic viscosity can be understand by considering the effect of the different viscosities on the velocity magnitude in the process mill by comparing the results of the simulation with high viscosity (30×10^{-3} Pa.s) and low viscosity (5×10^{-3} Pa.s) models.

Figure 41 summarises the results of the two simulations together with the reference model. The velocity distribution and magnitude does not differ significantly for the different viscosities as shown in Figure 41. This indicates that at rotational frequency of 600 rpm (10 revolutions per second) the effect of the ***studied dynamic viscosity*** of the drill cuttings on the velocity magnitude inside the process mill is minimal.

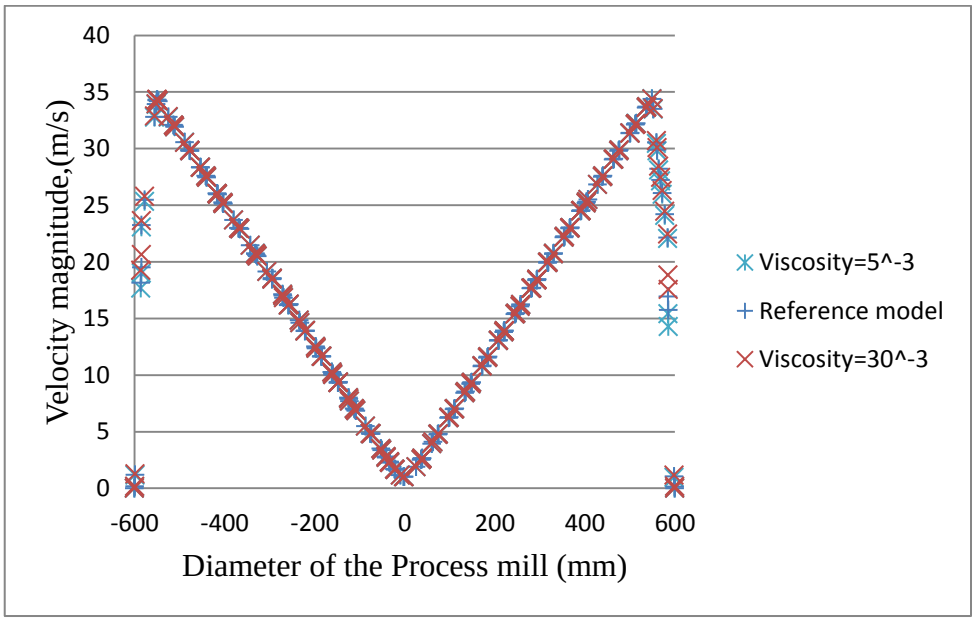

Figure 41 The velocity magnitude for models with varying dynamic viscosities

The heat generation by friction between the hammer tips and the drill cuttings inside the process mill drum may also contribute to the minimal effect observed for the dynamic viscosity, since viscosity decreases with increasing temperature.

2.7.4 Effect of the Thickness of the Hammers

Optimal hammer design and placement will provide maximum contact with drill cuttings. Also it will increase the friction between the hammer tip and the feed material which in turns increases the rate of heat generation in the process mill.

Two models of the process mill with different hammer thickness were simulated to study the effect of the thickness on the velocity magnitude and distribution in the process mill. Figure 42 **(a)** and **(b)** shows the effect of the hammer thickness on the velocity magnitude and distribution in the process mill.

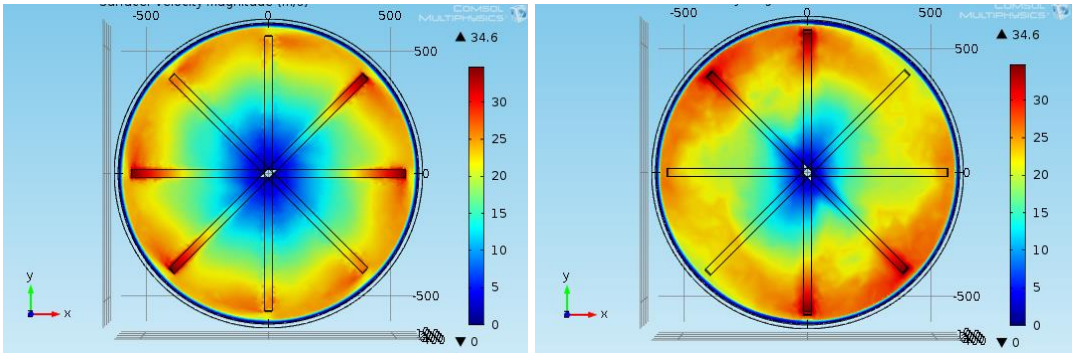

(a) Hammer thickness = 10 mm **(b)** Hammer thickness = 70 mm

Figure 42 The effect of the hammer thickness on the velocity distribution in the process mill

Impact is the primary force used in the hammer mill. Anything that increases the magnitude of the effective collision provides an advantage in particle size reduction. Increasing the magnitude of the effective collision between the hammer tips and the drill cuttings increases the rate of heat generation by friction in the process mill. Thus the hammer thickness is essential in the heat generation in the process mill.

It can be deduced from Figure 43 that, the 70 mm thick hammers have the least maximum velocity magnitude among the three models represented on the curve. It can be observed from Figure 43 that, the 10 mm thick hammers have a uniform velocity distribution which is much similar to the reference model's velocity distribution.

This reflects the similarities in the maximum velocity magnitude of the 10 mm thick hammers and the reference model (20 mm thick), which are 33.6 m/s and 33.9 m/s respectively. This make the 20 mm thick hammer (reference model) quite optimum.

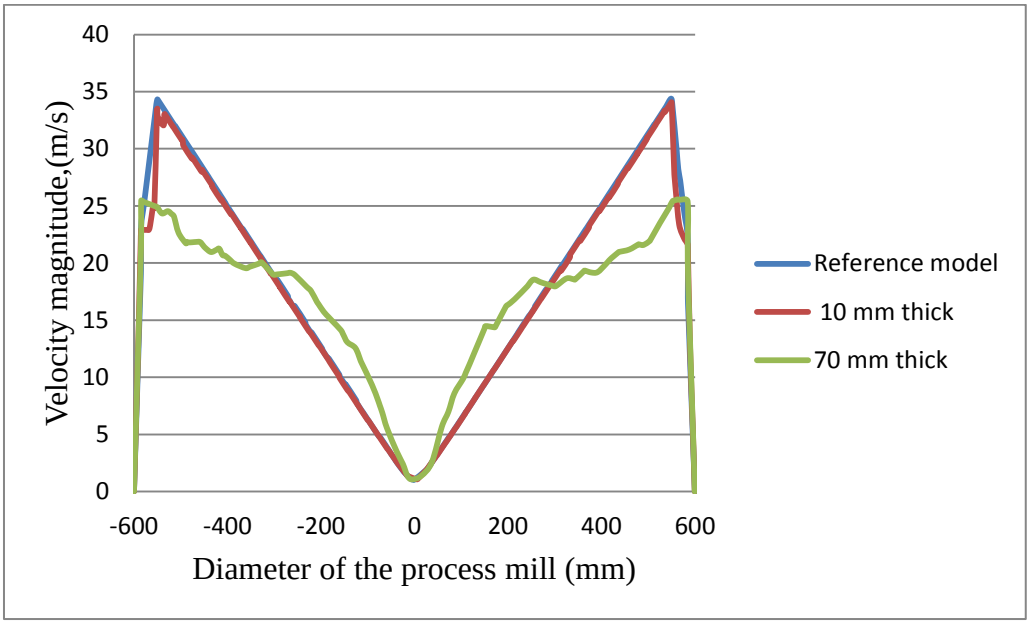

Figure 43 The effect of hammer thickness on the velocity magnitude

2.7.5 Effect of Angle between Adjacent Hammers

The angle between adjacent hammers is part of the arrangement of the hammers in the process mill, which contributes to its optimal operation. This simulation was done to study the effect of the angle between the adjacent hammers on the velocity distribution and the velocity magnitude inside the process mill.

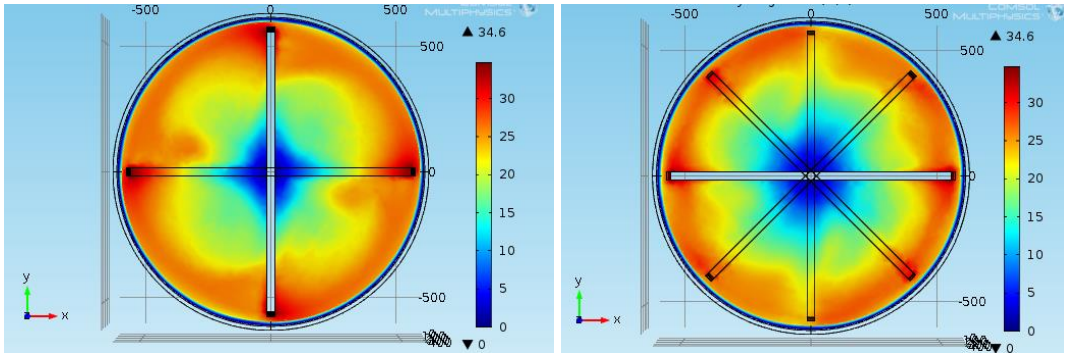

(a) Angle between hammers = 90 ^{o} **(b)** Angle between hammers = 45 ^{o}

Figure 44 The effect of the angle between adjacent hammers on the velocity distribution in the process mill

The velocity distribution is more uniform in Figure 44 **(b)** than in Figure 44 **(a)**. Comparing the model which has an angle of 90^{o} between the hammers to the reference model, it can be observed from Figure 45 that there is not much variation in the velocity magnitude. The model which has an angle of 90^{o} between the hammers recorded a maximum velocity magnitude of 34.14 m/s, while the reference model has a maximum velocity magnitude of 34.6 m/s. In addition, Figure 45 shows that the velocity magnitude for the model which has an angle of 90^{o} between the hammers was fluctuating along the radius of the hammer. It, however, increased steadily after 261 mm from the centre of the process mill. This fluctuation in velocity magnitude may be due to feed drop along the hammers, when they are arranged at 90^{o} adjacent to each other. The fluctuation in velocity magnitude may affect the heat generation process, which may in turns decrease the efficiency of the mill.

Figure 45 The effect of the angle between adjacent hammers on the velocity magnitude inside the process mill model

2.7.6 Effect of the Distance between Adjacent Hammers

The arrangement of the hammers in the process mill is essential to the optimal operation of the process mill. Even though the number of hammers a significant for efficient operation, the hammers should be balanced and arranged on the rotor so that they do not trail each other. This simulation was done to study the effect of the distance of separation between the hammers on the velocity distribution and the velocity magnitude inside the process mill.

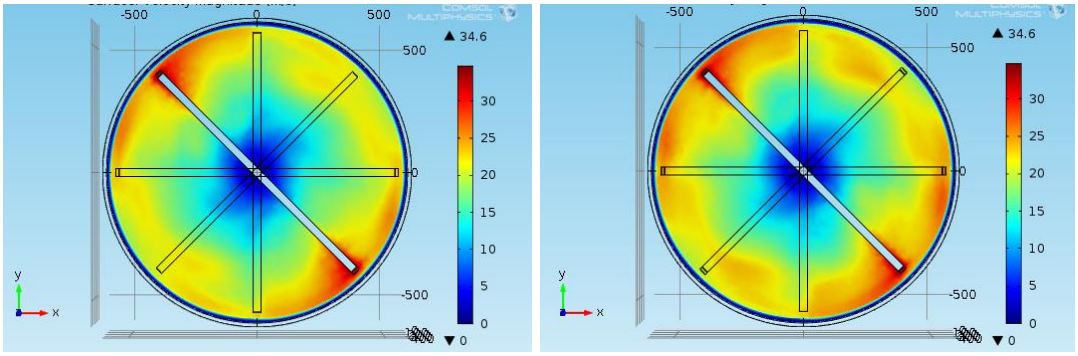

(a) Distance between hammers = 30 mm **(b)** Distance between hammers = 50 mm

Figure 46 The effect of the distance between adjacent hammers on the velocity distribution in the process mill

It can be observed that the velocity distribution is uniform in Figure 46 **(a)** and **(b)**. However, comparing the velocity magnitude to the reference model depicts that the velocity magnitude decreases with increasing the distance between adjacent hammers, as shown in Figure 47. The decrease in velocity magnitude will affect the rate of heat of heat generation in the process mill and hence decrease the efficiency. Therefore, it is better to design adjacent hammers with no distance between them.

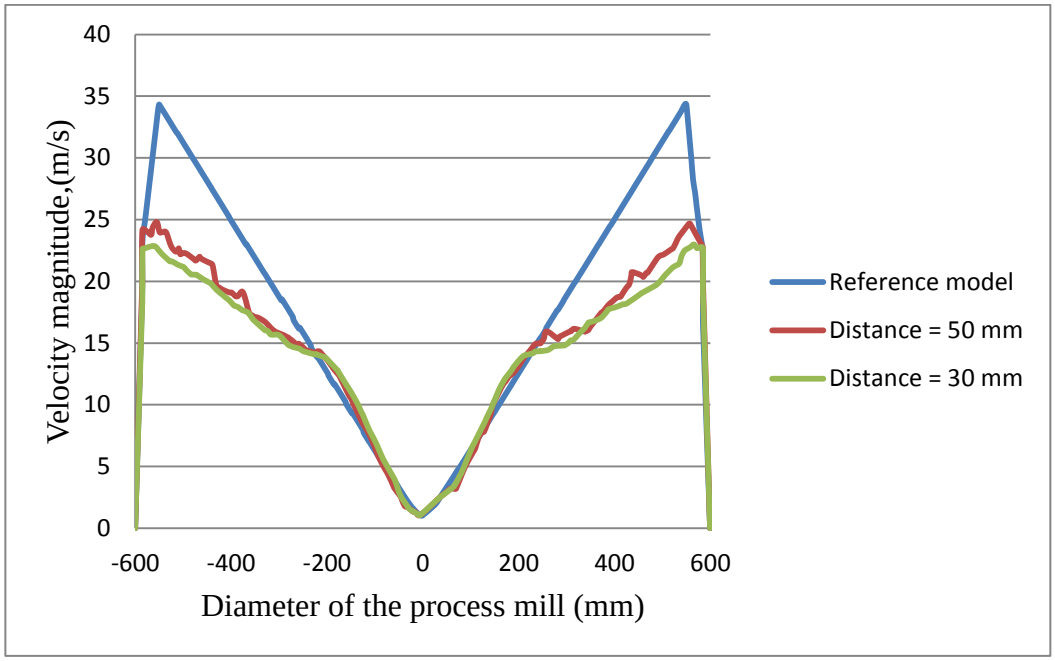

Figure 47 The effect of the distance between adjacent hammers on the velocity magnitude inside the process mill

2.8 CONCLUSION

The simulation and modelling of the process mill was an important task in this thesis work. This was done by varying some design, operating and process parameters and analysing their effect on the velocity distribution, velocity magnitude and the efficiency of the process mill.

It can be concluded that, the number of hammers is a vital design parameter to the velocity distribution inside the process mill. The 13 hammers in the reference model were found to be the optimum design compared to the 3 and 5 hammers in the case study. The model with 13 hammers gives the most uniform velocity distribution within the process mill.

The conclusion that can be drawn from analysing the results of the effect of the rotational frequency is that, the rotational frequencies have a minimal effect on the velocity distribution. This was observed at rotational frequencies above the critical mill speed. But below the mill's critical speed, it may have an effect on the velocity distribution. It could be a recommended issue for further work to simulate the effect of the rotational frequency when operating below the critical speed of the mill. However, the observed trend for increasing the rotational frequency from 10 rps to 100 rps confirms to theory: $= \pi \times D \times n$. Thus the velocity magnitude increased proportional to the rotational frequency.

The results confirms that, the effect of the range of viscosities studied is minimal compared to the reference model. This could be as a result of the high temperature inside the mill at operating conditions which may contribute to decreasing the viscosity of the feed material.

The fluctuation in the velocity magnitude observed for the design with adjacent hammers placed at 90 ^{o} to each other makes such design less optimal. This fluctuation may be due to fed drop and may affect the heat generation process hence decreasing the efficiency of the process mill. It can be concluded from this observation that, designing adjacent hammer such that they are at 45 ^{o} to each other is optimal compared to 90 ^{o}.

In addition, it can be concluded that optimal hammer design requires no distance in-between adjacent hammers. This was confirmed by the results from investigating the effect of the distance between adjacent hammers. The reference design, which has no distance between adjacent hammers, recorded the highest velocity magnitude (33.9 m/s) whereas a separation of 50 mm and 30 mm reduced the velocity magnitude to 24 m/s and 22 m/s respectively.

2.9 References

A. Brucato, M. Ciofalo, F. Grisafi, and G. Micale, *Numerical Prediction of Flow Fields in Baffled Stirred Vessels: A Comparison of Alternative Modeling Approaches*, Chemical Engineering Science, vol. 53, no. 21, pp. 3653–3684, 1998

G.K. Batchelor, *An Introduction to Fluid Dynamics*, Cambridge University Press, 2000.

H.P. Greenspan, *The Theory of Rotating Fluids*, Breukelen Press, 1990.

J.-P. Torré, D.F. Fletcher, T. Lasuye, and C. Xuereb, *Single and Multiphase CFD Approaches for Modelling Partially Baffled Stirred Vessels: Comparison of Experimental Data with Numerical Predictions*, Chemical Engineering Science, vol. 62, no. 22, pp. 6246–6262, 2007.

KLEPPE, S. *Re-using Recovered Base Oil from OBM Drilling Waste*. 2009.

3 CONCLUSIONS AND RECOMMENDATIONS

3.1 Substantial Conclusions from the Studies

Existing knowledge shows that, the hammer mill can handle a variety of feed types including drill cuttings which may consist of hydrocarbons, water, sand, rock particles and clay in an efficient manner to finer products. In addition, the energy that will be dissipated by the hammer mill to the milled product serves as the heating source for evaporating the hydrocarbons and water content of the drill cuttings. This way of using the dissipated heat makes the hammer mill the best mill type for the TCC process.

The elaborations from the studies show that COMSOL multiphysics is a good finite element tool to model and simulate the process mill. The mesh sensitivity shows that, fine mesh size and above was essential however, it increases the simulation time. A procedure was developed to accomplish the result of the simulations of the parameters of necessity.

Also a dependable procedure for simulating the response time of temperature change inside the process mill was devised. The findings from simulations showed that, with the exception of the process temperature, all the studied parameters have effect on the response delay. The observations made from this simulation showed that the effect on the response delay can be minimize by changing the parameters but cannot be eliminated.

The analysis of the simulation results in case study two shows that, hammer design (number of hammers, hammer thickness, distance and angle between adjacent hammers) is a critical parameter that affects the efficiency of the process mill. From the results of the simulations, it was observed that the velocity magnitude and distribution was mostly affected by hammer design. It can therefore be concluded that, for optimal operation of the process mill, the optimum hammer design must be reached which may not be limited to but including the number of hammers, hammer thickness, the angle and distance between adjacent hammers.

The findings obtained from the simulation shows that, the rotational frequency have a positive effect on the velocity magnitude. This was confirmed by the variation in velocity magnitude observed at rotational frequencies of 2, 10, and 100 revolutions per second which recorded velocity magnitudes of 6.91, 34.6 and 346 m/s respectively. This confirms the proportional relation between rotational frequency and velocity magnitude.

3.2 Recommendations for further Investigations

The effect of viscosity which was not observable in the simulation may be due to its negative correlation to increasing temperature, as the process mill operates at high temperatures. But with it being on the power or load, there was no prove because it was not covered in the scope of work. It is therefore recommend it as a topic for future investigation.

Finally, the effect of the rotational frequency on the velocity distribution when the process mill is operating below the mill's critical speed needs to be understood and hence recommended for future studies.